Geobios 77 (2023) 45–70

Contents lists available at ScienceDirect

Geobios

journal homepage: www.elsevier.com/locate/geobio

Original article

# The Mio-Pliocene transition in the Dacian Basin (Eastern Paratethys): Paleomagnetism, mollusks, microfauna and sedimentary facies of the Pontian regional stage ☆

Anton Matoshko [a,*], Arjan de Leeuw [b], Marius Stoica [c], Oleg Mandic [d], Iuliana Vasiliev [c,e], Alina Floroiu [c], Wout Krijgsman [a]

[a] Paleomagnetic Laboratory 'Fort Hoofddijk', Department of Earth Sciences, Utrecht University, Utrecht, Netherlands
[b] Institut des Sciences de la Terre (ISTerre), Université Grenoble Alpes, CNRS, IRD, 38000 Grenoble, France
[c] Department of Geology, Faculty of Geology and Geophysics, University of Bucharest, Bucharest, Romania
[d] Geological-paleontological Department, Natural History Museum Vienna, Vienna, Austria
[e] Senckenberg Biodiversity and Climate Research Centre (SBiK-F), Frankfurt am Main, Germany

ARTICLE INFO

*Article history:*
Received 21 September 2022
Revised 8 February 2023
Accepted 15 March 2023
Available online 28 March 2023

*Keywords:*
Late Miocene
Early Pliocene
Messinian
Zanclean
Deltaic deposits
Lacustrine deposits

ABSTRACT

Well-documented, high-resolution sedimentary sections are critical to our understanding of the often eventful evolution of semi-isolated basins that form during the final stages of continent–continent convergence, as exemplified by the Mediterranean-Paratethys system. Due to its nearly land-locked position in the Late Miocene, the Mediterranean experienced the renowned Messinian Salinity Crisis. At the same time, the equally restricted Eastern Paratethys to the north-east evolved in a potentially related, but very distinctive way. The events of this period are fully recorded in the sediments deposited during the Pontian regional stage in the Dacian Basin, part of the Eastern Paratethys, which we here investigate in detail in the best available section. The studied interval of the Slănicul de Buzău section is more than 2 km thick and almost continuously exposed. It is analyzed for paleomagnetism, mollusks, microfauna and sedimentary facies. This allows us to refine previous results from nearby but less complete sections, with particular improvements concerning resolution, biostratigraphy and sedimentology. The marine incursion just below the base of the Pontian (6.1 Ma) is shown to significantly predate the early Pontian highstand. The biostratigraphically defined onset of the middle Pontian (6.0 Ma) coincides with the highstand and slightly predates the major regression (5.9–5.6 Ma) for which the middle Pontian is best known. In the here-investigated section, the transgression at the beginning of the late Pontian (5.6 Ma) is followed by a regressive trend culminating between 5.4 and 5.2 Ma around the Mio-Pliocene boundary (5.33 Ma). The late Pontian sedimentation then becomes relatively stable and the fauna gradually transitions (4.8 Ma) into assemblages characteristic for the Dacian stage of the Dacian Basin, while overall significantly diverging from the rest of the Eastern Paratethys. Finally, we discuss several factors that could affect accuracy and applicability of the updated chronostratigraphy, warranting some caution.



## 1. Introduction

A string of semi-isolated basins may form during the final stages of continent–continent convergence. These basins can evolve in very striking ways in terms of base-level variations, sediment budgets, water-chemistry and faunal extinction, migration and radiation. To understand the often extremely rapid and eventful evolution of these basins, high resolution, well-dated sedimentary sections with detailed fossil records are critical.

A very good example of such a string of remarkable basins is the Mediterranean-Paratethys system, caught-up in the Africa-Eurasia convergence zone. The rise of the Alpine-Himalayan mountain chain in the Oligocene led to the differentiation of the epicontinental Paratethys Sea from the Tethys Ocean and its subsequent progressive fragmentation (Rögl, 1998; Popov et al., 2004). Connectivity between the different basins in the collision zone was limited to gateways and modulated by climate through the hydrological budget (Palcu and Krijgsman, 2022). As a result, the

☆ Corresponding editor: Frédéric Quillévéré.

* Corresponding author.
*E-mail address:* anton.matoshko@gmail.com (A. Matoshko).

https://doi.org/10.1016/j.geobios.2023.03.002
0016-6995/

history of the Paratethys realm shows a complex pattern of localized sea-level changes, salinity changes, faunal migration and endemism, significantly deviating from the World Ocean and the Mediterranean (Popov et al., 2006, 2010; Piller et al., 2007; de Leeuw et al., 2018; Palcu et al., 2021). This is reflected in a complicated relationship between a number of regional bio- and chronostratigraphic schemes requiring a multi-proxy approach for reliable correlation.

The Pontian stage in the Eastern Paratethys (Fig. 1(A)) received increased attention over the past three decades because of its correlation with the Mio-Pliocene transition (Vasiliev et al., 2004; Snel et al., 2006) and its overlap with the dramatic events of the Messinian Salinity Crisis (MSC) in the Mediterranean (Hsü et al., 1973; Roveri et al., 2014; Fig. 2). Due to good exposure, the Dacian Basin became the focus of integrated paleomagnetic and paleontological studies, which established a revised chronological framework for the Pontian (Vasiliev et al., 2004, 2005; Stoica et al., 2007, 2013; Krijgsman et al., 2010). Historically, the Eastern Paratethys response to the MSC was hypothesized as a major sea-level drop and desiccation based on deep-sea sediment cores and seismic sections, but onshore evidence suggests only a moderate regression (van Baak et al., 2017).

In this article we focus on the Pontian of the particularly continuous and fossiliferous Slănicul de Buzău section in the Dacian Basin (Fig. 1) and integrate sedimentary facies analysis, magnetostratigraphy, paleoecology, and biostratigraphy to arrive at a comprehensive paleoenvironmental record, which complements a number of earlier studies along other, less complete or more fragmentarily exposed sections (Vasiliev et al., 2004, 2005; Stoica et al., 2007, 2013; Krijgsman et al., 2010). Our work furthermore aims to complete the stratigraphic description of the Slănicul de Buzău section following the foregoing publications on its Sarmatian-Maeotian, Dacian and Romanian parts (van Baak et al., 2015; Jorissen et al., 2018; Lazarev et al., 2020).

Our sedimentological analyses can help discerning large-scale changes in depositional environment in this part of the Dacian Basin throughout the Miocene-Pliocene transition interval, supported by mollusk and ostracod range charts. The observed magnetostratigraphic polarity pattern allows to correlate the Pontian stage to the global timescale. While the long reversed chron C3r hampers high-resolution control on both Mediterranean and Paratethys geochronology in this time-interval, the ages of major shifts in depositional environments of the Dacian Basin, traditionally distinguished as the Odessian, Portaferrian and Bosphorian substage transitions, can be estimated assuming constant sedimentation rates. While magnetostratigraphic results, partly integrated with ostracod biostratigraphy, have been published from nearby sections before (Vasiliev et al., 2004, 2005; Stoica et al., 2013), Slănicul de Buzău undoubtedly presents the best opportunity for detailed stratigraphy of the Pontian in the eastern Dacian Basin, in terms of exposure and macro- and microfossil content, and thus deserves to be documented in detail.

## 2. Settings

### 2.1. The Pontian of the Eastern Paratethys

In the Late Miocene, the Eastern Paratethys included the Dacian Basin, Black Sea and Caspian Sea (Fig. 1). The latest Miocene to Early Pliocene Pontian regional stage was recognized in all three basins, although their internal division partly differs in nomenclature, content, and boundary definitions (Stevanović et al., 1989; Krijgsman et al., 2010; Rostovtseva and Rybkina, 2017; Popov et al., 2019). In the Dacian Basin, the Pontian stage is subdivided into lower, middle and upper intervals termed Odessian, Portaferrian and Bosphorian regional substages (Marinescu and Papaianopol, 1989). Their correlation with strata throughout the Paratethys and the Mediterranean is based on a detailed chronological framework (Krijgsman et al., 2010; Vasiliev et al., 2011; Rostovtseva and Rybkina, 2017; Fig. 2).

The lower Pontian (Odessian or Novorossian) is transgressive on Maeotian deposits (Popov et al., 2004, 2010). The Maeotian-Pontian transition is marked by a short influx of marine water with foraminifera observed throughout the Eastern Paratethys and dated around 6.1 Ma (Krijgsman et al., 2010; Stoica et al., 2013; Grothe et al., 2018; Van Baak et al., 2016a). High water levels during the early Pontian coincided with faunal migration from the Aegean and the Pannonian basins towards the Eastern Paratethys (Stevanović et al., 1989; Popov et al., 2006; Grothe et al., 2018). Simultaneously, Pontian Paratethys fauna migrated towards the Aegean (Gramann and Kockel, 1969; Krijgsman et al., 2020). The fluvio-deltaic system that occupied the East Carpathian Foreland during the Late Miocene was flooded and forced to retreat ~100 km inland at this time (de Leeuw et al., 2020).

The middle Pontian (Portaferrian; 5.8 ± 0.1–5.5 ± 0.1 Ma) is characterized by shallower environments in the Dacian Basin (Krijgsman et al., 2010; Stoica et al., 2013). Seismic data indicate a sea-level drop of ca. 100 m in the western Dacian Basin (Leever et al., 2010; Krézsek and Olariu, 2021) and continuous sedimentation in the Focşani Depression (Tărăpoancă et al., 2003; Krézsek and Olariu, 2021). Seismic data also reveal a hiatus on the Black Sea NW shelf and an accompanying lowstand systems tract in the contemporary deeper water area, both interpreted to correspond to the Portaferrian interval (Gillet et al., 2007; Munteanu et al., 2012; Krézsek et al., 2016). Note that the Portaferrian is a chronostratigraphic substage defined in the Pannonian Basin (Stevanović et al., 1989), with a different time extent than in the Dacian Basin. Nevertheless, we will use this regionally well-established name, because a revision of the Dacian Basin chronostratigraphic nomenclature is beyond the scope of the present study.

A second transgression occurred in the Dacian Basin at the base of the upper Pontian (Bosphorian), with an interpolated age of 5.5 Ma (Stoica et al., 2013), succeeded by mildly fluctuating environments in the Focşani Depression (van Baak et al., 2017). The top of the Bosphorian, i.e., the Pontian-Dacian boundary, was dated at 4.8 Ma in the Dacian Basin (Vasiliev et al., 2005; Krijgsman et al., 2010; Stoica et al., 2013; Jorissen et al., 2018). In the Topolog-Argeş area, situated along the South Carpathians, Odessian and Portaferrian deposits are missing, and Bosphorian transgressively overly Maeotian deposits (Stoica et al., 2007). The Bosphorian transgression is followed by progradation in the westernmost part of the Dacian Basin (ter Borgh et al., 2014).

Along the northern shore of the Black Sea (Kerch and Taman area), the upper Pontian is overlain unconformably by the Kimmerian. The lower part of the Kimmerian has a normal polarity interpreted to correspond to the Thvera subchron at ~5.2 Ma (Trubikhin, 1989; Krijgsman et al., 2010; Popov et al., 2016; Rostovtseva and Rybkina, 2017). This implies a shorter duration of the Pontian in the Black Sea basin than in the Dacian Basin. The Pontian-Dacian boundary in the Dacian Basin shows a gradual change in fauna and no prominent environmental shifts (Stoica et al., 2007). The Pontian in the Caspian Sea lasts at least until 5.4 Ma, being unconformably overlain by the fluvial Productive Series (Van Baak et al., 2016a).

Contrary to the Eastern Paratethys, the Pannonian Basin (Central Paratethys) was probably unaffected by any major sea-level changes during the Pontian (Magyar et al., 2013; Sztanó et al., 2013; ter Borgh et al., 2015; Kovács et al., 2021), although alternative interpretations exist (e.g., Csató et al., 2015).

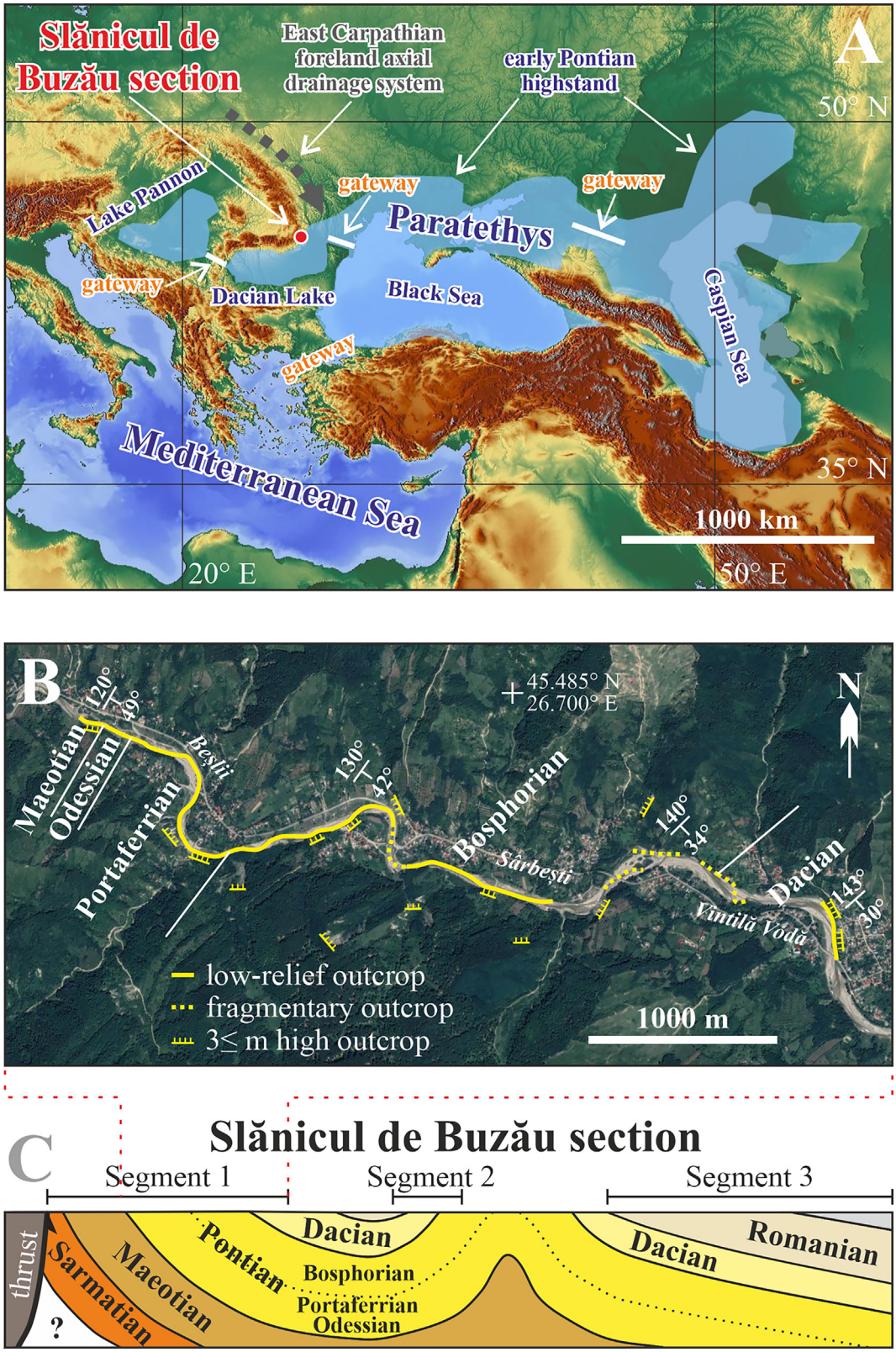


**Fig. 1.** Geographic and geological context of the Slănicul de Buzău section. **A.** Modern topography with overlay of the Paratethys paleogeography during the early Pontian highstand and possible locations of the gateways (modified after Popov et al., 2004; de Leeuw et al., 2020). **B.** Studied interval on a satellite image (Google, CNES/Airbus) in the context of the whole Slănicul de Buzău section along the Slănic River (**C**).

### *2.2. The Late Miocene to Pliocene climate*

Latest Miocene (7–5.4 Ma) global sea surface temperatures reflected the culmination of a cooling trend that approached near modern values before temporary reversal of these trends in the Early Pliocene (Herbert et al., 2016). This global climatic cooling was associated with transient glaciations in Greenland (Larsen et al., 1994) and distinctive glacial-to-interglacial cycles in the

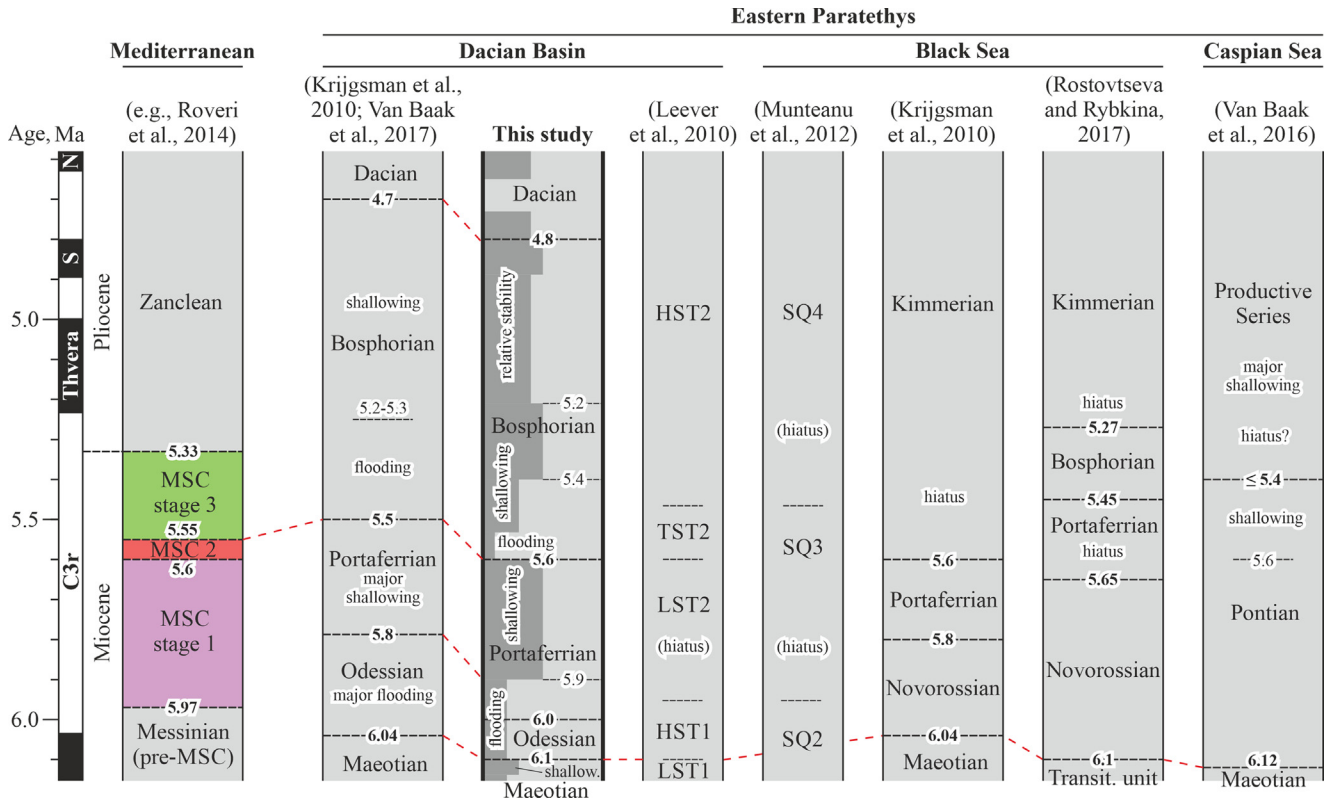


**Fig. 2.** Stratigraphic table depicting latest chronostratigraphy and sequence stratigraphy in the Eastern Paratethys and Mediterranean.

North Atlantic from 6.26 to 5.5 Ma (Hodell et al., 2001). This suggests that a marked deglaciation occurred at 5.5 Ma, predating the Mio-Pliocene boundary (5.33 Ma) by ~170 kyr, and potentially corresponding to the Bosphorian transgression.

A positive hydrological budget is estimated for the Paratethys in the Late Miocene from climate modeling due to its vast northern drainage basin (Marzocchi et al., 2016). Highly evaporative conditions are on the other hand suggested for the Black Sea during the middle Pontian based on geochemical indicators (Vasiliev et al., 2013, 2015).

### 2.3. The Dacian Basin and the Slănicul de Buzău section

The Dacian Basin is the part of the Carpathian foreland basin that stretches from Romania into Serbia and Bulgaria. It formed in the Middle to Late Miocene (Badenian-Sarmatian) during the final stages of foreland propagating thrusting (Bertotti et al., 2003). In the earliest Late Miocene, with the disintegration of the Central Paratethys and the establishment of Lake Pannon in the Pannonian Basin System, the Dacian Basin waterbody became part of the Eastern Paratethys. The Focşani Depression was a major foreland depocenter that accumulated up to 13 km of sediments from Middle Miocene to Recent and underwent prominent post-collisional subsidence (Bertotti et al., 2003; Tărăpoancă et al., 2003; Krézsek and Olariu, 2021). It was supplied mainly from the North by the axial drainage system of the East Carpathian foreland (de Leeuw et al., 2020; Krézsek and Olariu, 2021). The western flank of the Focşani Depression was incorporated in the Carpathian wedge and strongly tilted during the Late Miocene-Pleistocene (Tărăpoancă et al., 2003; Leever et al., 2006; Matenco et al., 2007) without significant horizontal-plane rotation (Dupont-Nivet et al., 2005).

The latter tilting and uplift led to a marked incision of the rivers that have thus exposed a number of km-long sections, among which the Slănicul de Buzău section. This is a composite section through the limbs of a syncline-anticline pair thus consisting of three major segments (Fig. 1(C)). The section exposes roughly 6 km of Upper Miocene, Pliocene and Lower Pleistocene deposits, attributed to the Khersonian, Maeotian, Pontian, Dacian and Romanian regional stages. The Romanian (van Baak et al., 2015), Dacian (Jorissen et al., 2018) and Khersonian to Maeotian (Lazarev et al., 2020) intervals of the section were recently studied in detail, while this paper is focused on the remaining Pontian interval (Fig. 1(B)).

We here investigate a ~2200 m-thick stratigraphic interval starting in the uppermost Maeotian, spanning the whole Pontian and ending in the lower part of the Dacian. Along this interval, bedding planes gradually shallow from 120°/49° to 143°/30° (azimuth/dip). Most of the exposure occurs in 1–3 m high undercut river banks, the river bed and sometimes in the neighboring cliffs. The section is almost continuously exposed, but does change from year to year as a function of landslides and river floods, which leads to a highly variable level of observable details. Exposures of the river bed are particularly variable.

## 3. Material and methods

The studied section represents interfingering of 0.01–10 m thick fine sandstones (or sands) and 0.01–70 m thick muds (silts, clays). Sampling for magneto- and biostratigraphy was focused on muds, while some mollusk samples were also taken from sandstones. The whole spectrum of lithologies was subjected to facies analysis.

### 3.1. Magnetostratigraphy

One hundred fifty paleomagnetic levels were drilled in the here investigated part of the Slănicul de Buzău section using a portable electrical drill powered by a generator. Two cores were taken per

sampling level and all samples were oriented in the field using a dedicated stage and compass. A local declination correction of 5° (https://www.ngdc.noaa.gov) was added to the sample orientations to compensate for secular variation.

Paleomagnetic measurements were made at Paleomagnetic laboratory "Fort Hoofddijk", Utrecht University, the Netherlands. Samples were demagnetized thermally (TH), or through an alternating magnetic field (AF) to establish the characteristic remanent magnetization (ChRM). During thermal demagnetization, samples were stepwise heated with increments of 30–40°C up to 680°C, or to a lower temperature if the remanent magnetization became less than 10% of its initial value. After each temperature step, the remanent magnetization was measured in multiple positions on a horizontal 2G Enterprise DC SQUID cryogenic magnetometer (noise level $3\times10^{-12}$ $Am^2$). Alternating field demagnetization was accomplished on a robotized handler controller attached to a horizontal 2G Enterprise DC SQUID cryogenic magnetometer (Mullender et al., 2016). Samples were gradually demagnetized in alternating field (AF) with a strength from 0 to 100 mT with increments of 2–20 mT and their remanent magnetization was automatically measured after every field increment. Demagnetization diagrams and intensities are diverse, hinting at the presence of a variety of magnetic carriers throughout the section and sometimes even within a single sample (Fig. 3).

### 3.2. Biostratigraphy and paleoecology

#### 3.2.1. Mollusks

Forty-nine mollusk samples, each containing up to 3 kg of fossiliferous mud or sandstone, were taken along the section between the years 2011 and 2016. Their preparation was carried out in the geological-paleontological department of the Natural History Museum Vienna.

The overall preservation of the shells is poor. They are heavily fragmented and in general cannot be properly separated from the sediment. Each mollusk sample was first hand-picked for the most complete specimens, after which the sediment boulders were carefully split to smaller pieces to gain as much determinable material as possible. Each extracted specimen was cleaned, as far as possible, from the matrix by means of hand-chisels, vibro-tools and sand-blasting devices. Finally, the specimens were conserved, where necessary, with a diluted vinyl acetate aqueous dispersion. The residual material was dried and set overnight in a 3% $H_2O_2$ solution and then washed over a 1 mm mesh-size sieve and hand-picked under the microscope. The study material is stored in the collection of the Geological-Paleontological Department of the Natural History Museum Vienna.

Taxonomic identifications of the mollusk fauna and its paleoecological and biostratigraphic interpretations follow the current mollusk literature on the Upper Miocene and Lower Pliocene of the Paratethys, such as Stefanescu (1896), Wenz (1942), Andreescu (1977), Marinescu (1977), Papaianopol (1989, 1995), Iljina et al. (1976), Stevanović et al. (1989), Nevesskaja et al. (1986, 1997, 2001), Stoica et al. (2007, 2013), and references therein. Taxonomic classification and synonymy follows MolluscaBase (2023) except for *Amygdalia* Nevesskaja et al., 2013, which we consider for a junior synonym of *Coelogonia* Bronn, 1837, and *Pachyprionopleura* Andreescu, 1974, which we consider for a valid taxon different from *Prosodacna* Tournouër, 1882. Altogether, 78 taxa from 4748 specimens have been identified at species or genus level (Table S1, Appendix A).

#### 3.2.2. Microfauna

In addition, 190 microfossil samples were taken. Microfossils were analyzed at the Faculty of Geology and Geophysics of the University of Bucharest following a standard methodology (Stoica et al., 2013). The samples consisted of 0.5–1 kg of mud, which was dried, boiled in a sodium carbonate solution and washed through an array of sieves (63–500 μm). Microfossils were picked under a microscope and stored in cell-slides. In general microfossils were moderately preserved.

Taxonomic identification of ostracods and their biostratigraphic significance follow mainly the works dedicated to Paratethyan ostracods studies such as Livental (1929), Schneider (1949), Schweyer (1949), Suzin (1956), Agalarova et al. (1961), Mandelstam and Schneider (1963), Agalarova (1967), Karmishina (1975), Hanganu (1974), Hanganu and Papaianopol (1982), Vekua 1975, Krstic and Stancheva (1989), Olteanu (1979, 1989a,b, 1995), Sokač (1972, 1989, 1990), Stancheva (1968, 1990), Stoica et al. (2013, 2016), Gliozzi (1999), Gliozzi et al. (2005), Cziczer et al. (2009), Floroiu et al. (2011), Popov et al. (2016), van Baak et al. (2016a), Richards et al. (2018), Spadi et al. (2019), Lazarev et al. (2020), Rausch et al. (2020) and references therein.

In order to reconstruct the paleoecological preferences of ostracod species, we used the literature dedicated to the ecology of "recent" ostracod faunas like in the works of Yassini (1986), Danielopol et al. (1990), Meisch (2000), Horne et al. (2012), Karanovic (2012), Williams et al. (2018), Briceag et al. (2019), applied by Olteanu (2006), Gliozzi and Grossi (2004, 2008), Rostovtseva and Tesakova (2009) to fossil species with Paratethyan affinities.

### 3.3. Sedimentary facies analysis

The heterogeneity in the details available for observation and the enormous length of the section imposed a simplified approach for the facies analysis, focusing on readily distinguishable ubiquitous features. These include lithology, sedimentary structures, mollusk shells content and color. The section shows several 0.1–70 m-thick repetitive groups of sedimentary features described as facies associations and interpreted to represent major depositional environments. On the scale of 60–600 m these facies associations are generalized into facies units which underline longer duration sedimentary trends.

## 4. Results

### 4.1. Magnetostratigraphy

During thermal demagnetization, a small viscous component (20–100°C) was removed first (Fig. 4(A, B)). There was subsequently often a low temperature component present in the 100–225°C interval, which generally had a direction resembling the Present-day magnetic field in geographic coordinates, or in other cases a direction intermediate between that and the subsequent third component. The third component occurred in the 225–400°C interval (Fig. 4(B)). Only two samples showed a distinctive high temperature component in the 400–600°C interval (Fig. 4(C)).

Alternating field demagnetization diagrams generally reveal a first, low field component between 0–25 mT, which is easily distinguished from the subsequent higher field component(s) and frequently shows a direction resembling the Present-day field in geographic coordinates. We interpret this component to reflect a recent overprint. In most cases, there is subsequently a consistent second component in the 25–60 mT interval (Fig. 4(D)). Most samples still retained a significant part of their initial intensity at 60 mT. However, in roughly half of the samples weak to prominent gyroremanence was observed in the 60–100 mT field interval (Fig. 4(E)), suggesting the presence of an iron sulphide and obscuring any higher coercivity component present. The other half of the samples continued to demagnetize, in the 60–100 mT interval

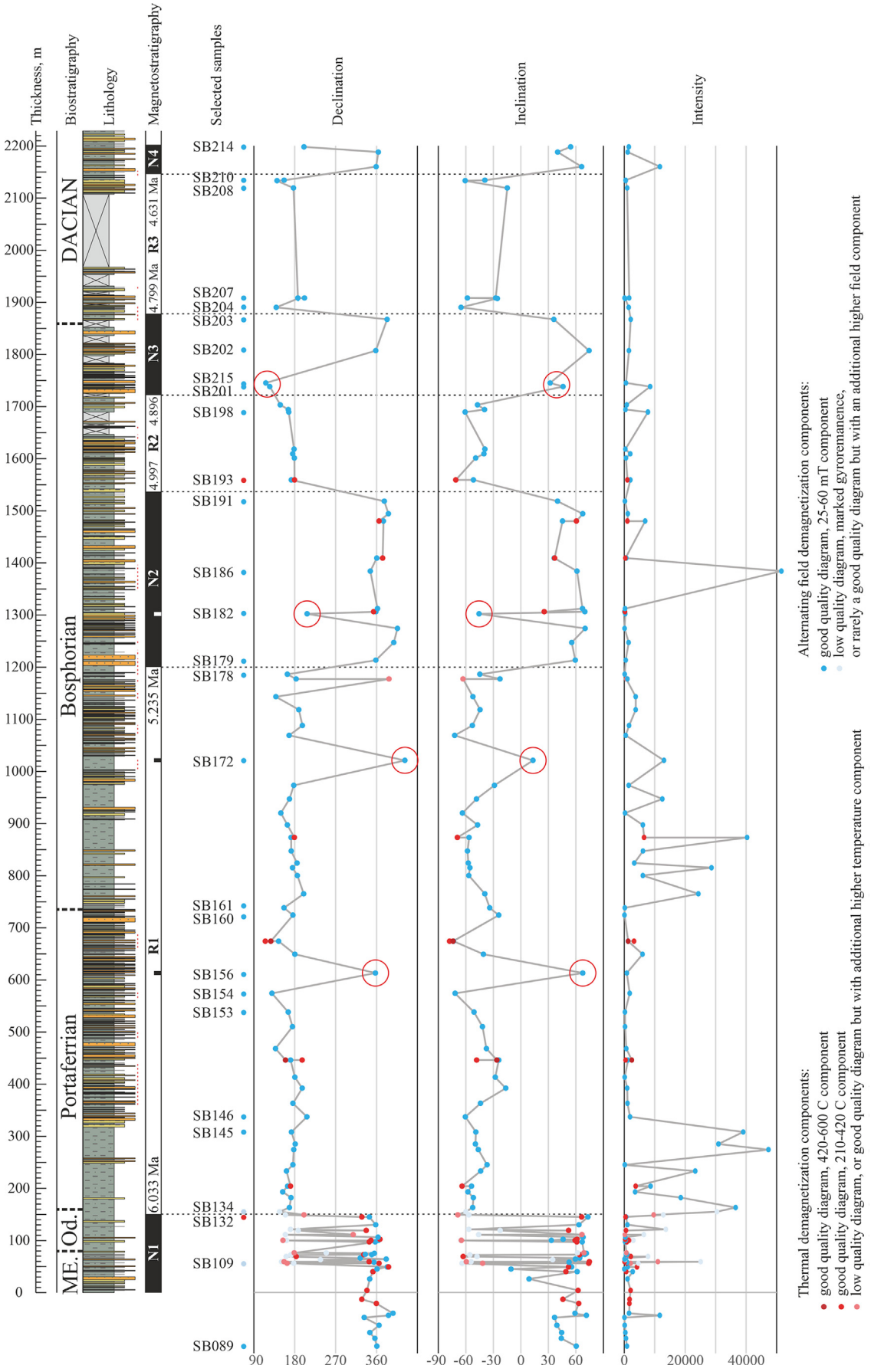


**Fig. 3.** Palaeomagnetic polarity pattern identified in the Slănicul de Buzău section.

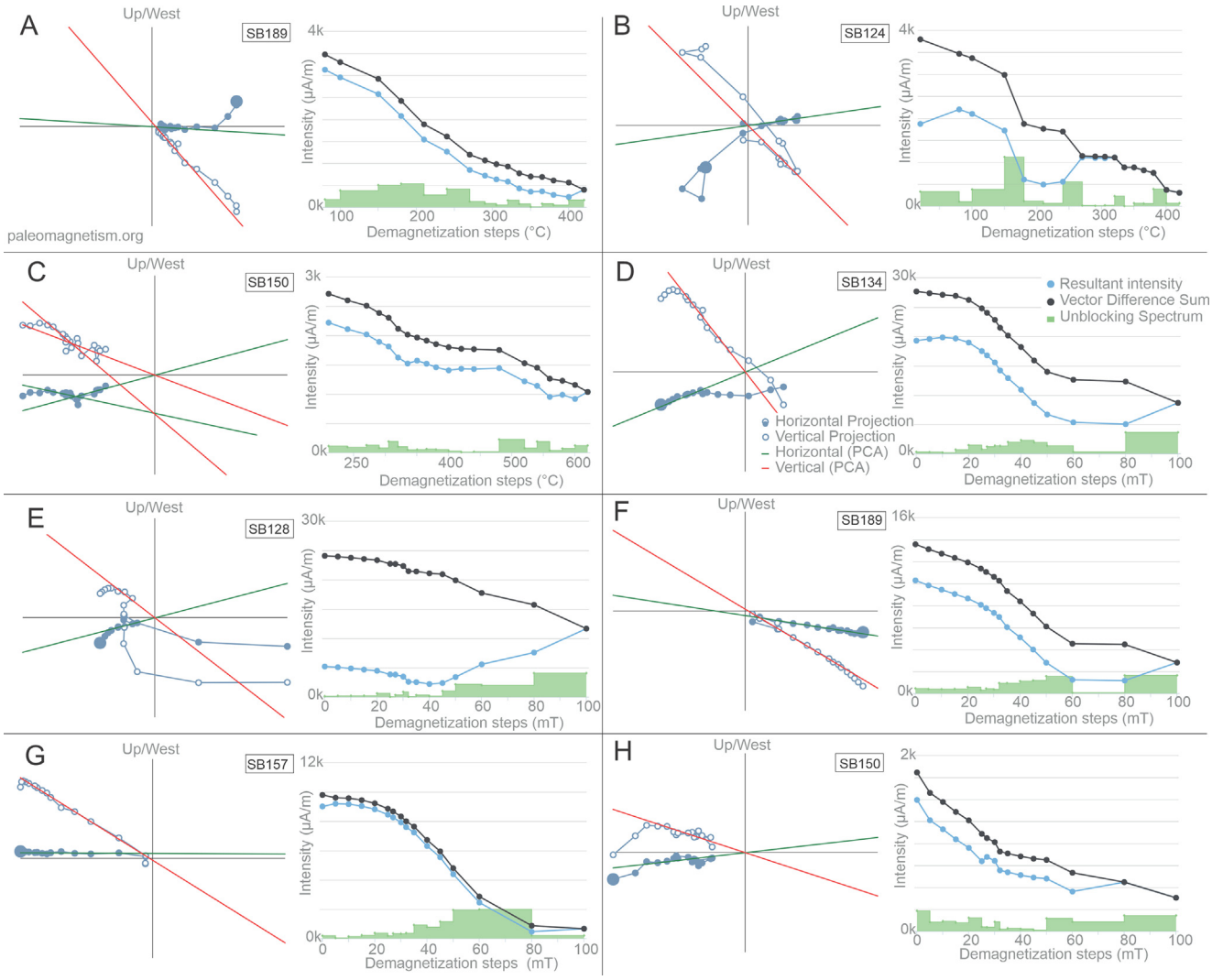


**Fig. 4.** Zijderveld diagrams and intensity diagrams for representative samples from the Pontian of Slănicul de Buzău. All Zijderveld diagrams are in tectonic coordinates. Figures made with paleomagnetism.org.

(Fig. 4(F, G)), generally with a direction similar to the one observed in the 25–60 mT interval. Very few samples have a high-coercivity component that is not completely demagnetized at 100 mT (Fig. 4 (C, H) provides thermal demagnetization diagram for the same sample).

Our paleomagnetic results allow to establish a magnetostratigraphic polarity pattern (Fig. 3). The directions of the identified 225–400°C and 400–600°C as well as the 25–60 mT, 60–100 mT components show both normal and reverse directions in tectonic coordinates. The directions cluster better in tectonic than in geographic coordinates and cluster on logical average normal and reverse field directions. Even though these are nearly antipodal, they do not strictly have a common true mean direction (Tauxe, 2010). This is, however, commonly observed in Paratethys sediments that usually show large sets of directions based on a combination of magnetite and greigite directions that define very narrow averages (Vasiliev et al., 2011; Van Baak et al., 2016b; Palcu et al., 2021). Our paleomagnetic results show seven polarity intervals, which can be straightforwardly correlated to the geomagnetic polarity timescale (Raffi et al., 2020; Fig. 3).

The only interval where the polarity may be disputed is the interval between samples SB109 and SB132, which exhibits frequently alternating normal and reversed directions. Sometimes there are opposing directions for two magnetic components in a single sample, with the higher temperature component generally being of normal polarity. In our opinion, this reflects an early diagenetic downward replacement of some normal polarity directions by reversed ones, which thus places the C3An.1n–C3r reversal at the top of this interval and in the Odessian (Fig. 3). However, this implies that the reversal coincides with a sharp change in magnetic mineralogy, as indicated by the sudden increase in intensity (Fig. 3), which is slightly suspicious. However, placing the reversal at the base of this interval is more problematic as this would imply a high-temperature overprint with a normal direction in tectonic coordinates (the strata are significantly tilted), which would be difficult to explain. On the basis of the currently available information, we thus prefer to place the C3An.1n–C3r reversal at the top of the interval with frequently alternating polarities, in the Odessian.

### 4.2. Biostratigraphy and paleoecology

The Pontian is defined biostratigraphically and further subdivided into the Odessian (lower Pontian), Portaferrian (middle Pontian) and Bosphorian (upper Pontian) substages based on mollusk and ostracod first occurrences. In particular, we here follow the


A
B
C
D
E
F
G
H
I
J
K
L
M
N
O
P
Q
R
S
T
U
V
W
X
Y
Z
AA
AB
AC
AD
AE
AF
AG
AH
AI
AJ
AK
AL
AM
AN

original definition provided by Marinescu and Papaianopol (1989) for the Pontian stage and substages. The rich mollusk (Figs. 5–7) and ostracod (Figs. 8–10) fauna of the Slănicul de Buzău section allows to readily distinguish these substages.

*4.2.1. Mollusks*

*4.2.1.1. Upper Maeotian-Odessian.* The Maeotian interval is represented by two samples (Fig. 7). The lower sample comprises a monospecific assemblage of *Dreissenomya rumana* with articulated shells (Table S1, Appendix A). This species is restricted to the upper Maeotian of the Dacian Basin (Marinescu, 1977). The second sample follows ~40 m upwards and comes from a densely packed shell bed dominated by disarticulated shells of *Coelogonia pseudorostriformis,* all oriented parallel to the bedding. *Coelogonia pseudorostriformis*, previously known as *Congeria novorossica navicula*, is a marker of the topmost Maeotian in the Dacian Basin (Marinescu and Papaianopol, 1989). Both the shallow infaunal *Dreissenomya* and the epifaunal byssate *Coelogonia* were brackish water dwellers (Iljina et al. 1976). Their monospecific presence and dominance probably indicate a stressed environment (Brenchley and Harper, 1998).

The Odessian interval is represented by the subsequent three samples (Fig. 7). It is marked by a dominance of *Pseudoprosodacna littoralis* ssp., followed by partially abundant *Pseudocatillus pseudocatillus*, *Pontalmyra novorossica*, *Dreissena* (*Pontodreissena*) *rostriformis corniculata*, *Dreissena* (*Modiolodreissena*) *rimestiensis*, and *Hydrobia spicula* (Table S1, Appendix A). All the cardiid taxa show their first appearance in the Odessian, supporting the corresponding biostratigraphic correlation (Nevesskaja et al., 1986). The mollusk assemblage composition of these samples, dominated by cardiids, points to a deep littoral depositional environment. Moreover, the specific cardiid genera that occur, are able to survive nearly freshwater conditions, which might indicate fluctuating brackish to freshwater conditions in this interval (Nevesskaja et al., 2001).

*4.2.1.2. Portaferrian.* The onset of the Portaferrian interval is marked by the lowermost occurrences of *Congeria* (*Rhombocongeria*) *rhomboidea* and *Caladacna steindachneri* in the studied section (Fig. 7; Table S1, Appendix A). In the Eastern Paratethys, *C.* (*R.*) *rhomboidea* is restricted to the Portaferrian, while *C. steindachneri* first appears in this interval but persists later on (Nevesskaja et al., 1986; Stevanović et al., 1989). The four samples from the lower, mud-dominated part of Portaferrian furthermore contain *Congeria* (*Rhombocongeria*) *unica*, *Chartoconcha candida*, *Tauricardium petersi*, and *Prosodacnomya sabbae*. Whereas *C.* (*R.*) *unica* is confined to the Portaferrian, the other species occur in the Bosphorian as well (Papaianopol, 1975; Andreescu, 1977; Stevanović et al., 1989; Nevesskaja et al., 1997). In more detail, this interval starts with abundant *Caladacna*, replaced in its middle part by *Paradacna*, subsequently followed by *Euxinicardium* and *Dreissena* (*Modiolodreissena*) (Fig. 7). Whereas *Paradacna* indicates deep water conditions, the other three taxa are shallow water, littoral markers (Nevesskaja et al., 2001). Shallow littoral representatives, such as *Hydrobia*, *Lithoglyphus* or *Dreissena* are increasingly rare in this interval, while additional deep water indicators such as *Chartoconcha* or *Valenciennius* occur more frequently. This reflects a short-term shift from deep littoral to deeper profundal conditions. The taxonomic composition with an increased number of Lake Pannon taxa, such as *Caladacna*, *Paradacna*, *Chartoconcha*, *Tauricardium*, *Congeria* (*Rhombocongeria*) and *Valenciennius*, points to a stable mesohaline salinity in this interval (~12 ppm; Stevanović et al., 1989).

There subsequently is a marked change in the mollusk fauna, which coincides with a switch to sandier deposits (Fig. 7). In this interval, all previously mentioned brackish-water taxa are absent, whereas *Hydrobia*, *Lithoglyphus*, *Dreissena*, and *Prosodacnomya* in turn become very abundant (Fig. 7). There are also some new elements, such as *Theodoxus*, *Viviparus*, *Rumanunio*, and *Melanopsis*, that also become very abundant. This mollusk assemblage is characteristic for shallow littoral environments. The persistent occurrence of viviparids and unionids suggests lowered or fluctuating salinity levels. This interpretation is supported by the presence of euryhaline neritids and melanopsids (Iljina et al., 1976).

*4.2.1.3. Bosphorian.* The Portaferrian-Bosphorian boundary is marked by the lowermost occurrences of *Pseudocatillus subzalatarskii*, *Parapachydacna cobalcescui*, and *Prosodacna semisulcata*, followed by *Zagrabica reticulata* slightly above (Fig. 7; Table S1, Appendix A). All of these species have their first occurrences in the Bosphorian, but only *Pseudocatillus subzalatarskii* occurs exclusively in this substage (Stevanović et al., 1989; Nevesskaja et al., 1997; Macalet, 2002). The mollusk assemblage in the lower ~300 m of the Bosphorian includes frequent deep-water taxa *Paradacna*, *Valenciennius*, and *Chartoconcha*, indicative of open-lake mesohaline conditions in a deep littoral setting (Nevesskaja et al., 1986). The great abundance of *Paradacna* in the lowermost Bosphorian suggests an even deeper, profundal environment. Abundant *Pontalmyra* and *Euxinicardium* subsequently indicate a deep littoral setting (Nevesskaja et al., 2001), shortly interrupted by a sample with shallow littoral markers.

In the middle part of the Bosphorian (1030–1310 m interval) the mollusk assemblage becomes very similar to the one from the sand-dominated part of the Portaferrian, with predominant *Theodoxus*, *Prosodacnomya*, *Dreissena*, *Melanopsis*, and *Viviparus* in varying proportions. Euryhaline *Prosodacna* and *Parapachydacna,* which have their first occurrence in the lower part of the Bosphorian, do nevertheless remain abundant in this interval. The mid-Bosphorian mollusk assemblage indicates a nearly freshwater, shallow littoral depositional setting.

There are subsequently a number of typical first occurrences in the upper part of the Bosphorian, including those of *Stylodacna*

**Fig. 5.** Cardiid bivalve species from the study section with indicated sample number. **A**. *Dacicardium vetustum* Papaianopol, 1983, ME16/69. **B**. *Dacicardium* cf. *rumanum* (Fontannes, 1887), ME16/78. **C**. *Euxinicardium botenicum* (Papaianopol, 1983), ME16/97. **D**. *Euxinicardium inlongaevum* (Eberzin, 1947), ME13/40. **E**. *Euxinicardium nobile* (Stefanescu, 1896), ME13/28. **F**. *Euxinicardium sacrum* (Papaianopol, 1983), ME16/96. **G**. *Euxinicardium* cf. *moskoni* (Papaianopol, 1983), ME16/68. **H**. *Tauricardium petersi* (Hoernes, 1862), ME16/96e. **I**. *Paradacna abichi* (Hoernes, 1874), ME13/27. **J**. *Paradacna* cf. *blandita* Papaianopol, 1978, ME16/62. **K**. *Phyllocardium planum* (Deshayes, 1838), ME16/63. **L**. *Pontalmyra gratiosa* Papaianopol, 1981, ME13/28. **M**. *Pontalmyra subcarinata* (Dashayes, 1838), ME16/70. **N**. *Pontalmyra novarossica* (Barbot de Marny, 1869), ME13/24. **O**. *Pontalmyra* cf. *ovata* (Deshayes, 1838), ME16/97. **P**. *Pseudocatillus motasi* Papaianopol, 1984, ME16/62. **Q**. *Pseudocatillus subzalatarskii* (Eberzin, 1967), ME16/65. **R**. *Pseudocatillus pseudocatillus* (Abich in Barbot de Marny, 1869), ME13/25. **S**. *Pseudocatillus* aff. *sokolovi* (Vassoevich and Eberzin, 1930), ME16/67. **T**. *Pseudocatillus* cf. *corbuloides* (Deshayes, 1838), ME16/63. **U**. *Pseudocatillus* cf. *bellus* (Papaianopol, 1981), ME16/97. **V**. *Chartoconcha bayerni* (Hoernes, 1874), ME16/64. **W**. *Chartoconcha rumana* (Wenz, 1942), ME16/69. **X**. *Chartoconcha candida* Papaianopol, 1975, ME13/28. **Y**. *Chartoconcha minuta* Papaianopol, 1975, ME16/95. **Z**. *Caladacna steindachneri steindachneri* (Brusina, 1884), ME13/26. **AA**. *Caladacna steindachneri controversa* Papaianopol, 1978, ME16/62. **AB**. *Pseudoprosodacna littoralis littoralis* (Eichwald, 1850), ME13/25. **AC**. *Pseudoprosodacna littoralis plicatolittoralis* (Sinzov, 1897), ME16/64. **AD**. *Pseudoprosodacna littoralis* morph. *semisulcatoides* (Eberzin, 1959), ME13/24. **AE**. *Prosodacnomya rostrata* (Sinzov, 1900), ME13/29. **AF**. *Prosodacnomya sabbae* Andreescu, 1977, ME16/71. **AG**. *Prosodacna semisulcata* (Rousseau, 1842), ME16/97. **AH**. *Prosodacna* cf. *fischeri* Davidaschvili, 1931, ME16/81. **AI**. *Prosodacna* cf. *macrodon minor* Andrusov, 1917, ME16/64. **AJ**. *Pachydacna* (*Parapachydacna*) *cobalcescui* (Fontannes, 1887), ME16/97. **AK**. *Stylodacna heberti* (Cobalcescu, 1883), ME16/81. **AL**. *Pachyprionopleura* cf. *munieri munieri* Stefanescu, 1896, ME16/95. **AM**. *Pachyprionopleura* cf. *munieri orolesi* Papaianopol, 1984, ME16/98. **AN**. *Plagiodacna* cf. *angulosa* (Deshayes, 1857), ME16/63. Scale bars: 5 mm.

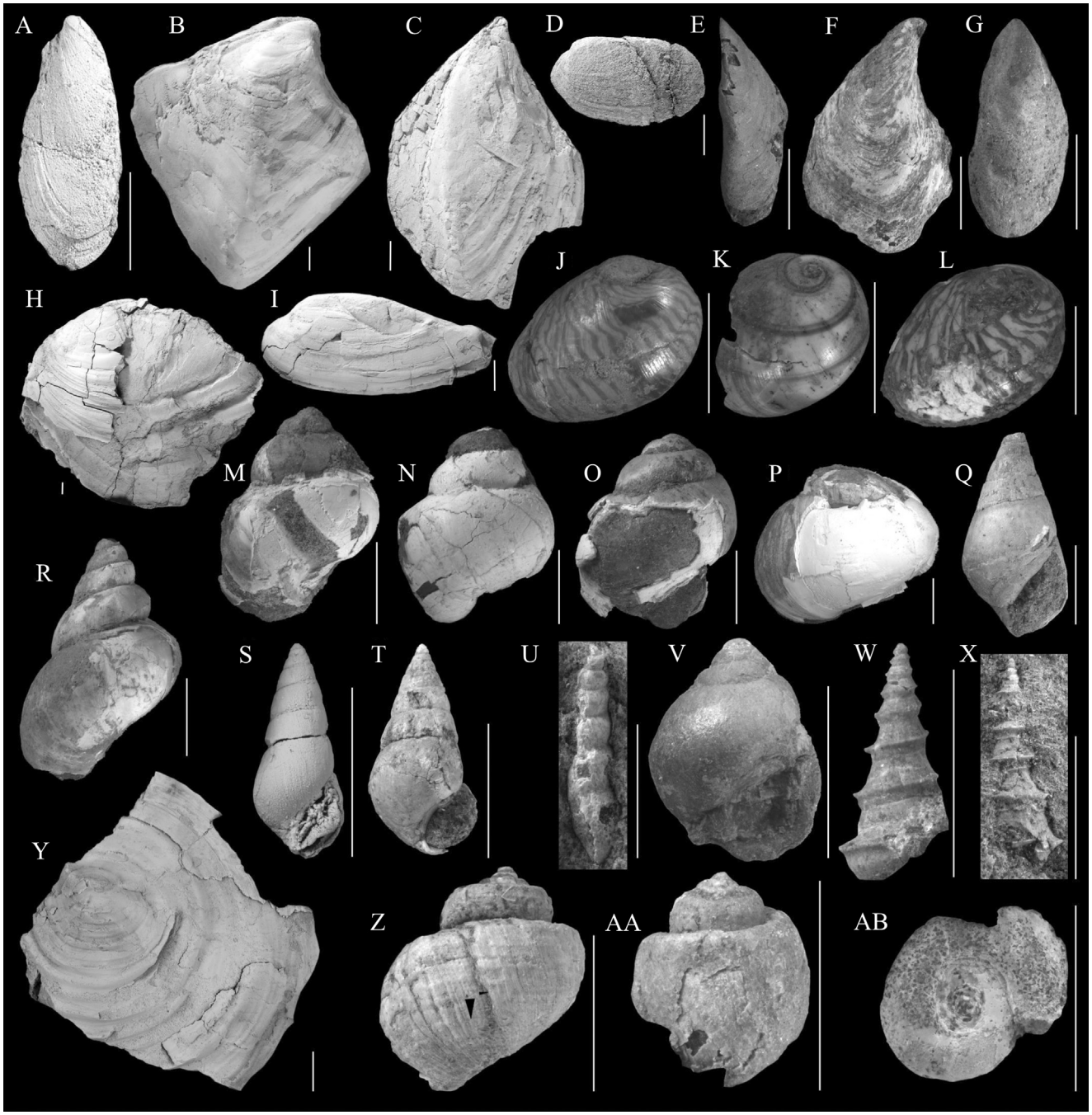


**Fig. 6.** Bivalve (dreissenids and unionids) and gastropod species from the study section with indicated sample number. **A**. *Coelogonia pseudorostriformis* (Sinzov, 1897), ME13/22. **B**. *Congeria* (*Rhombocongeria*) *rhomboidea* Hoernes, 1867, ME13/26. **C**. *Congeria* (*Rhombocongeria*) *unica* Papaianopol and Macalet, 1998, ME13/26. **D**. *Dreissenomya rumana* (Wenz, 1942), ME13/21. **E**. *Dreissena tenuissima* Sinzov, 1875, ME13/31a. **F**. *Dreissena* (*Pontodreissena*) *rostriformis corniculata* Stefanescu, 1896, ME16/63. **G**. *Dreissena* (*Modiolodreissena*) *rimestiensis* Fontannes, 1887, ME13/28. **H**. *Hyriopsis krausi* (Wenz, 1932), ME13/31a. **I**. *Rumanunio rumanus* (Tournouër, 1879), ME13/31a. **J**. *Theodoxus galeatus* (Marinescu, 1962), ME16/74. **K**. *Theodoxus quadrifasciatus* (Bielz, 1864), ME13/36. **L**. *Theodoxus scriptus* (Stefanescu, 1896), ME13/30. **M**. *Viviparus achatinoides* (Deshayes, 1838), ME16/73. **N**. *Viviparus botenicus* Lubenescu and Zazuleac, 1985, ME13/32. **O**. *Viviparus wesselinghi* Neubauer, Harzhauser, Georgopoulou, Mandic and Kroh, 2014, ME13/37. **P**. *Viviparus* cf. *papaianopoli* Lubenescu and Zazuleac, 1985, ME13/40. **Q**. *Melanopsis decollata* Stoliczka, 1862, ME16/71. **R**. *Tylopoma speciosa* (Cobălcescu, 1883), ME16/63. **S**. *Hydrobia pontilitoris* Wenz, 1942, ME13/33. **T**. *Hydrobia spicula* Stefanescu, 1896, ME16/73. **U**. *Prososthenia* cf. *radmanesti* (Fuchs, 1870), ME16/66. **V**. *Lithoglyphus rumanus* Stefanescu, 1896, ME13/31a. **W**. *Pyrgula boteniensis* Wenz, 1942, ME13/37. **X**. *Pyrgula* cf. *atava* Brusina, 1881, ME16/97. **Y**. *Valenciennius annulatus* Rousseau, 1842, ME16/80. **Z**. *Zagrabica carinata* Andrusov, 1909, ME16/79. **AA**. *Zagrabica reticulata* Stefanescu, 1896, ME16/75. **AB**. *Gyraulus rumanus* Wenz in Krejci-Graf and Wenz, 1932, ME16/96. Scale bars: 5 mm.

*heberti*, *Euxinicardium sacrum*, *Chartoconcha minuta*, and *Pachyprionopleura* cf. *munieri orolesi*. It is remarkable that these could be detected despite the low-quality mollusk record of this interval, which allowed determination of only a restricted number of specimens (Fig. 7). With exception of *S. heberti*, all latter species are restricted to the Bosphorian, i.e., they disappear at the onset of the Dacian (Papaianopol, 1975, 1983, 1984; Pană et al., 1981). Following its first occurrence in the Bosphorian, *S. heberti* becomes common in the Dacian (Andreescu, 1977).

In paleoecological terms, the above described assemblage from the upper part of the Bosphorian is marked by the re-occurrence of the deep-water representative *Valenciennius* at 1318 m (Fig. 7). The

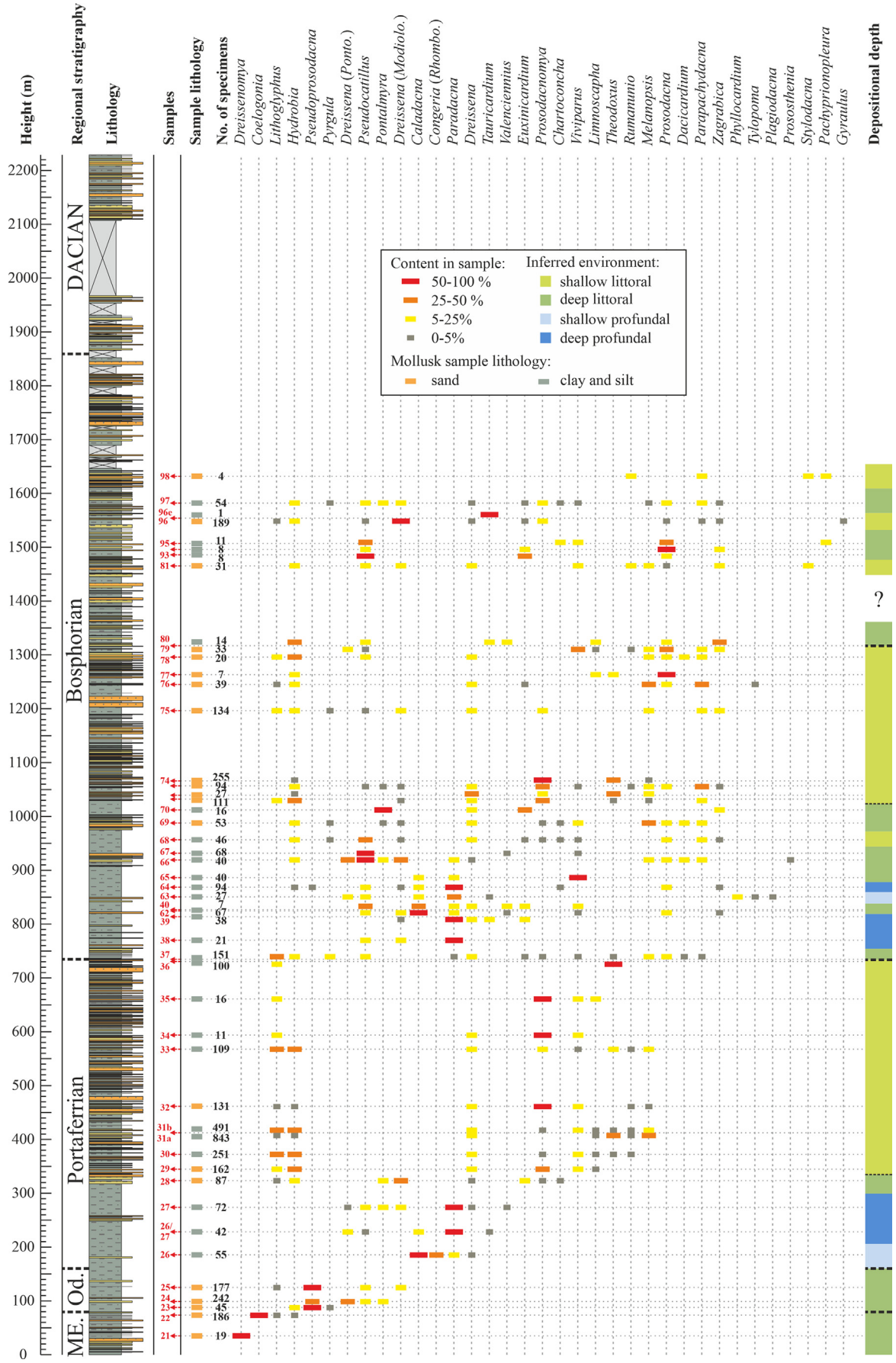


**Fig. 7.** Position of mollusk samples in the section with indicated lithology, their genus-level content with plotted abundances, and the resulting paleodepth interpretation (see text for details).

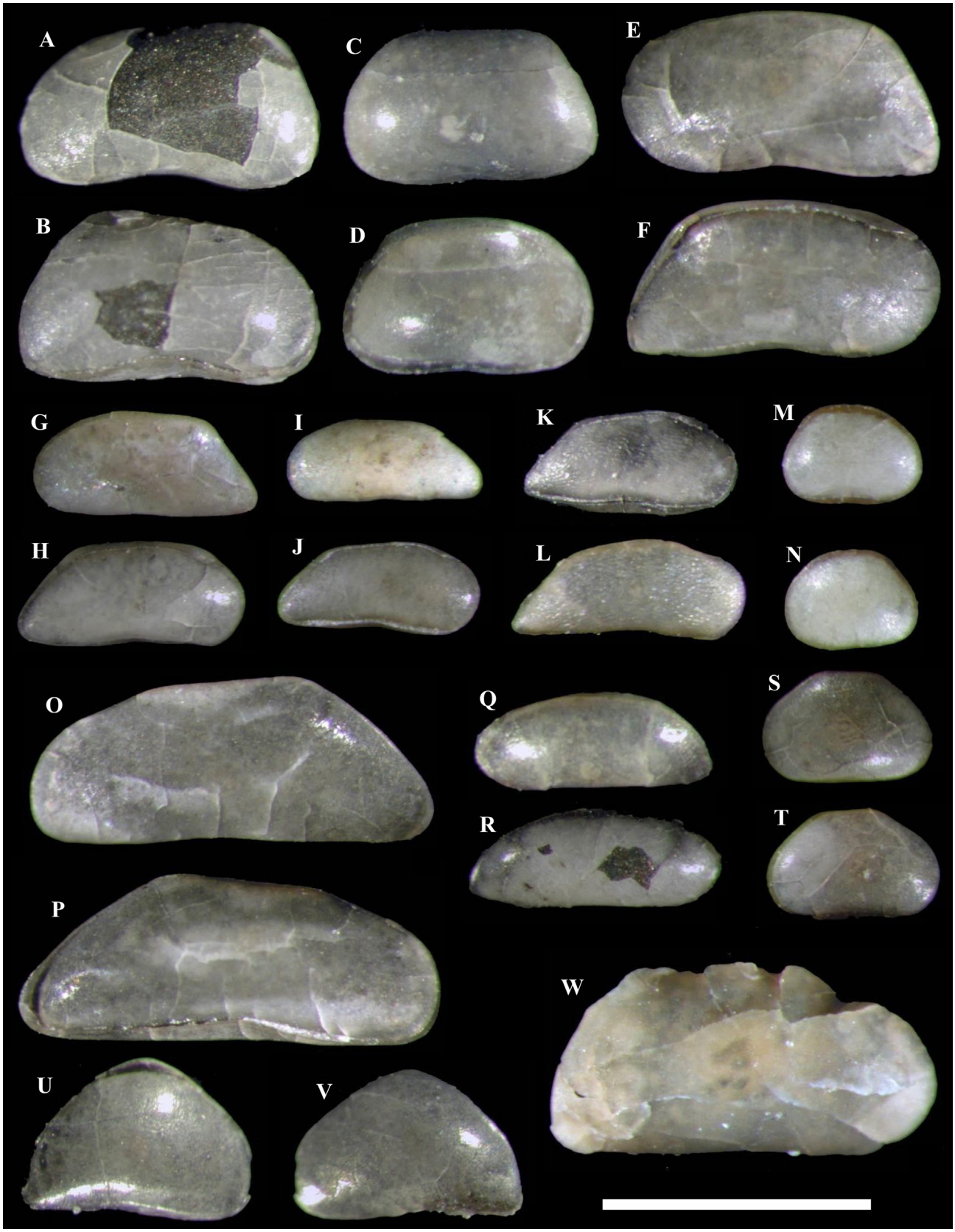


**Fig. 8.** Common ostracods from the Pontian in the Slănicul de Buzău section. **A, B**. *Candona* (*Caspiocypris*) *pontica* Sokač, 1972. **C, D**. *Candona* (*Caspiocypris*) *alta* (Zalányi, 1929). **E, F**. *Candona* (*Camptocypria*) *ossoinaensis* Krstić, 1969. **G, H**. *Pontoniella ex. gr. quadrata* (Krstić, 1969). **I, J**. *Pontoniella acuminata* (Zalányi, 1929). **K, L**. *Pontoniella acuminata* (Zalányi, 1929) var. *striata* (Mandelstam, 1963). **M, N**. *Cypria tocorjescui* Hanganu, 1962. **O, P**. *Candona* (*Hastacandona*) *loczyi* (Zalányi, 1929). **Q, R**. *Candona* (*Zalanyiella*) *venusta* (Zalányi, 1929). **S, T**. *Cypria* sp. 1. **U, V**. *Typhlocypris* sp. **W**. *Amplocypris dorsobrevis* Sokač, 1972. Scale bar: 1 mm.


**Fig. 9.** Common ostracods from the Pontian in the Slănicul de Buzău section. **A-D**. *Bakunella dorsoarcuata* (Zalányi, 1929). **E, F**. *Cyprideis* ex. gr. *torosa* (Jones, 1850). **G, H**. *Pontoleberis pontica* (Stancheva, 1965). **I-L**. *Tyrrhenocythere filipescui* (Hanganu, 1962). **M, N**. *Cytherissa bogatschovi* Livental, 1929. **O, P**. *Cytherissa* ex. gr. *bogatschovi* (Livental, 1929). **Q-T**. *Amnicythere andrusovi* (Livental, 1929). **U, V**. *Euxinocythere cornutocostata* (Schweyer, 1949). **W, X**. *Amnicythere cymbula* (Livental, 1929). **Y, Z**. *Amnicythere sinegubi* (Krstić, 1975). **AA, AB**. *Amnicythere multituberculata* (Livental, 1929). **AC, AD**. *Maeotocythere* ex. gr. *bosqueti* (Livental, 1929). **AE, AF**. *Loxoconcha petasa* Livental, 1929. **AG-AJ**. *Loxoconcha babazananica* Livental, 1929. Scale bar: 1 mm.

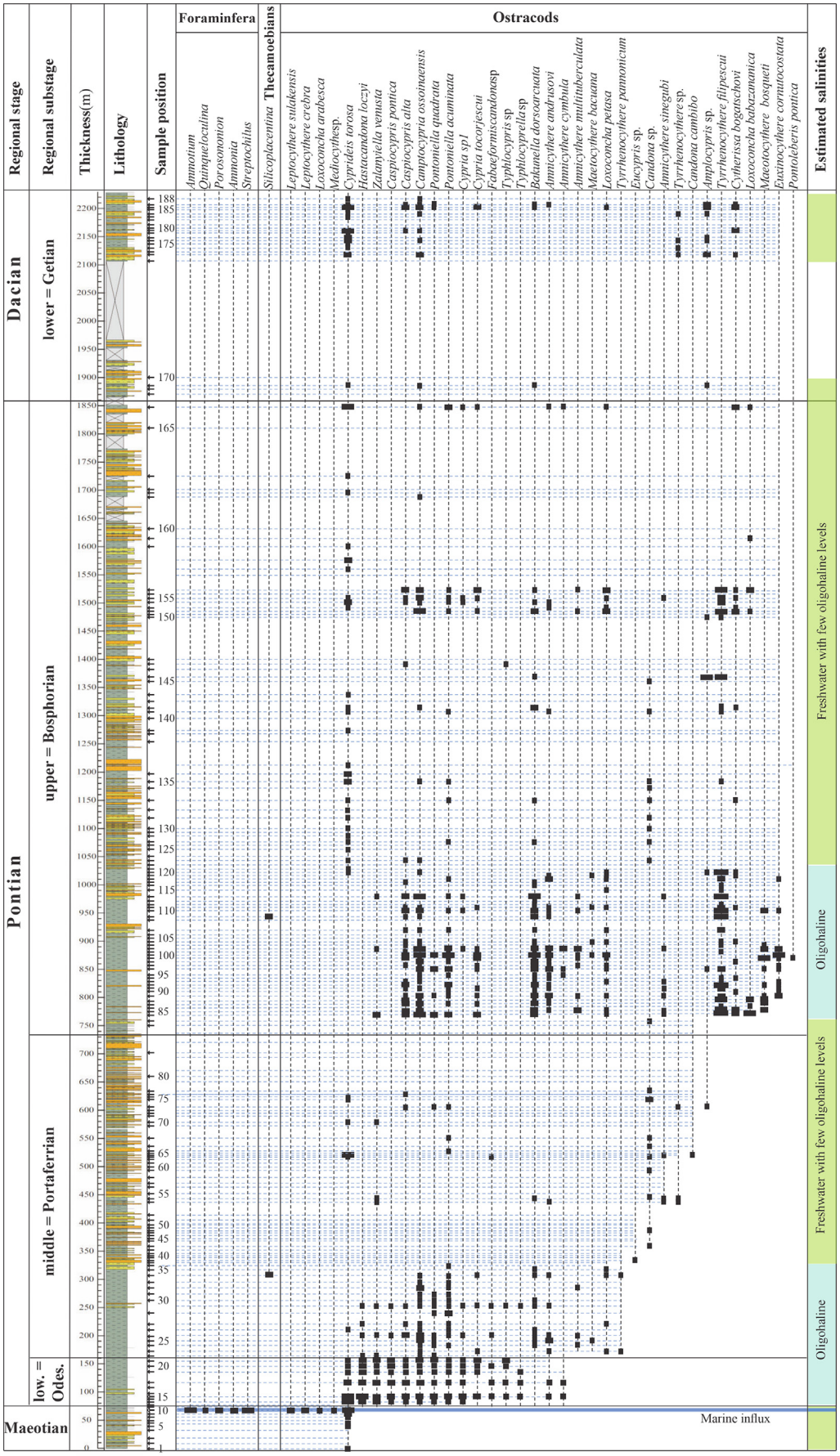


**Fig. 10.** Position and content of microfauna samples in the Slănicul de Buzău section (see text for details).

presence of *Chartoconcha* similarly points to deep-water brackish conditions (Nevesskaja et al., 2001). Nevertheless, most of the samples in this interval have increased abundances of taxa indicating deep littoral brackish conditions such as *Pseudocatillus*, *Euxinicardium*, *Prosodacna*, *Tauricardium*, *Stylodacna*, and *Pachyprionopleura,* suggesting the depositional environment remained slightly shallower than in the lower part of the Bosphorian. However, the frequent presence of *Rumanunio*, *Limnoscapha*, *Viviparus*, *Valvata*, and *Gyraulus* clearly points to a fresh water input and occasionally decreased salinity. The punctual increase in abundance of the shallow littoral markers such as *Hydrobia* furthermore indicates some water-level fluctuations (Wilke et al., 2000).

*4.2.2. Microfauna*

*4.2.2.1. Upper Maeotian-Odessian.* The ostracod assemblage of the uppermost Maeotian is dominated by *Cyprideis torosa*, topped by a thin interval with a significant admixture of marine foraminifera. This is followed by the appearance of many new species of Candonidae and some Cytheridae ostracods characterizing the Odessian interval (Figs. 8, 10). They include: *Candona* (*Caspiocypris*) *pontica*, *Candona* (*Caspiocypris*) *alta*, *Candona* (*Hastacandona*) *loczyi*, *Candona* (*Camptocypria*) *ossoinaensis*, *Candona* (*Zalanyiella*) *venusta*, *Pontoniella quadrata*, *Pontoniella acuminata*, *Cypria* sp. 1, *Cypria tocorjescui*, *Typhlocypris* sp. and *Amnicythere andrusovi*. Several ostracods like *Cyprideis torosa*, *Fabaeformiscandona* sp., *Typhlocyprella* sp. and *Amnicythere cymbula* persist into the Odessian from the uppermost Maeotian. In the lowermost Odessian there is a thin marker interval with pyritized ostracods. Overall, ostracods are indicative of an oligohaline (∼7‰) environment by comparison with related extant taxa as outlined in the methods section.

*4.2.2.2. Portaferrian.* The Portaferrian is marked by the first occurrences of *Bakunella dorsoarcuata*, *Amnicythere multituberculata*, *Maeotocythere bacuana*, *Loxoconcha petasa* and *Tyrrhenocythere pannonicum* (Figs. 9, 10). Ostracods like *Candona* (*Hastacandona*) *loczyi*, *Candona* (*Caspiocypris*) *pontica*, *Typhlocyprella* sp. and *Tyrrhenocythere pannonicum* occur for the last time in this interval. Finally, there is a single sample with *Silicoplacentina majzoni*, brackish thecamoebians. The ostracods of this interval suggest an increase in depth with respect to the underlying Odessian.

There is subsequently a very marked change in the ostracod assemblage, which goes hand in hand with a switch to sand-dominated sedimentary facies. This interval is characterized by a lack of ostracods in many samples or the exclusive presence of juveniles of *Candona* sp., which indicates subaerial to ephemeral freshwater environments. Some samples nevertheless reveal a more diverse ostracod assemblage including *Cyprideis torosa*, *Candona* sp., *Pontoniella acuminata*, *Candona* (*Zalanyiella*) *venusta*, *Candona* (*Caspiocypris*) *alta*, rarely *Pontoniella quadrata*, *Fabaeformiscandona* sp., *Bakunella dorsoarcuata* and *Amnicythere andrusovi*. A few ostracods such as *Amnicythere sinegubi* and *Amplocypris* sp. appear for the first time in this interval, while *Fabaeformiscandona* sp. occurs for the last time. Rare finds of *Candona cambibo* and *Eucypris* sp. are limited to this interval. The ostracods in this interval are indicative of freshwater to oligohaline conditions (0-4‰) by comparison with related extant taxa as outlined in the methods section.

*4.2.2.3. Bosphorian.* The Bosphorian interval begins with an ostracod bloom including many species that persisted from the Odessian (Figs. 8–10): *Candona* (*Caspiocypris*) *alta*, *Candona* (*Camptocypria*) *ossoinaensis*, *Candona* (*Zalanyiella*) *venusta*, *Pontoniella quadrata*, *Pontoniella acuminata*, *Cypria* sp. 1, *Cypria tocorjescui*, *Bakunella dorsoarcuata*, *Amnicythere andrusovi*, *Amnicythere cymbula*, *Amnicythere multituberculata*, *Amnicythere sinegubi*, *Maeotocythere bacuana*, *Loxoconcha petasa* and *Amplocypris* sp. There are in addition several new Cytheridae ostracods, which did neither occur in the Odessian nor in the Portaferrian: *Tyrrhenocythere filipescui*, *Cytherissa bogatschovi*, *Loxoconcha babazananica*, *Maeotocythere bosqueti* and *Euxinocythere cornutocostata*. Some ostracods are found exclusively in the basal part of Bosphorian interval: *Candona* (*Zalanyiella*) *venusta*, *Maeotocythere bacuana*, *Maeotocythere bosqueti* and *Euxinocythere cornutocostata*. There furthermore is a single sample with *Silicoplacentina majzoni* thecamoebians. The overall diverse assemblage of ostracods indicates oligohaline (∼7‰) conditions for this interval by comparison with related extant taxa as outlined in the methods section.

The initial ostracod bloom is succeeded by an interval (1030–1400 m) with a much lower ostracod abundance and diversity. Euryhaline *Cyprideis torosa* and freshwater *Candona neglecta* are prominent in this generally impoverished interval. This suggests freshening (0–4‰) and a more proximal environment, although some sporadic brackish-water indicative species do occur once in a while, suggesting some fluctuation in the paleoenvironment. Above 1400 m sampling density decreases, which precludes a detailed view of the potential environmental fluctuations in the upper Bosphorian. There is however a clear bloom in ostracod diversity and abundance in the 1470–1530 m interval. The relative diversity and abundance of ostracods in eight successive samples in this interval indicates more stable, brackish-water conditions. The onset of this bloom is, on the other hand, poorly constrained due to a lack of samples in the 1400–1470 m interval of the section. The ostracod bloom is followed by another low abundance, low diversity interval although the lower sampling density does not allow conclusive evaluation. The investigated part of the Dacian interval in any case does not show any significant changes in ostracod assemblage in comparison with the upper Bosphorian. The most notable change is the lack of *Tyrrhenocythere filipescui*.

### 4.3. Sedimentary facies analysis

*4.3.1. Facies associations*

The multiple observations of various sedimentary features showed that some of them have greater diagnostic value than others. The most distinctive features served as the basis for identification of the facies associations (see Table 1 for full list of features). The interpretation of their depositional environments emerges from a holistic view of facies relationship in the section and existing depositional models (Reading, 1996; Bridge and Demicco, 2008).

The most readily distinguishable facies association is characterized by abundant mollusk shells occurring in largely structureless, up to 70 m thick muds and generally up to 0.3 m thick sandstones (Fig. 11). These features suggest relatively slow deposition and bioturbation in a standing body of water with sufficient time and appropriate conditions for mollusks to live and accumulate. In the context of the Dacian Basin this environment is identified as lake-dominated. It can be roughly differentiated into shoreface (thin sandstones) and offshore (muds).

The lake-dominated facies frequently interfinger with another distinct facies association that consists of generally well-bedded sandstones with common indicators of unidirectional flow, particularly current cross-lamination, and laminated muds, lacking mollusk shells and comprising classical coarsening upwards parasequences 2–10 m thick (Fig. 12(A–G)). It can be interpreted to have accumulated in result of progradation of a shallow delta lobe, subsequently abandoned and replaced by apparent lake transgression. Its sandstones can be assigned to the delta front while the muds pertain to the prodelta. The rarity of wave-induced and the absence of tide-induced sedimentary structures allow to identify the delta as river-dominated. Close analogs of

such shallow delta parasequences were observed in the river-dominated part of the Dunvegan delta (Bhattacharya, 2010).

The shallow delta facies association needs to be differentiated from a similar association comprising the upper part of parasequences differing by poor stratification in sandstones, lack of bedforms and much larger proportion of underlying lake-dominated muds. This coarsening upward facies association consists of crude parallel bedded virtually structureless sandstones (Fig. 12(H, I)) and laminated muds similar to prodelta facies. It implies more abrupt deposition, tentatively interpreted as turbidite, while stratigraphic proximity to the shallow delta suggests a possible hyperpycnal mechanism of flow initiation.

The shallow delta facies are in some cases overlain by a facies association characterized by structureless mottled muds with coaly layers and sandstones with thick irregular bedding, prominent erosive surfaces and indicators of unidirectional flow, overall lacking mollusk shells, 0.1–50 m thick (Fig. 13). These features indicate relatively slow deposition of muds in oxidizing subaerial to reducing mire conditions on a floodplain and rapid deposition of sandstones in channels or their proximity (i.e., crevasse splay, levee). This facies association is identified as delta top.

#### 4.3.2. Facies unit types

The distinguished facies associations each pertain to a specific part of the sedimentary system, including delta top (proximal), shallow delta (intermediate), lake-dominated (distal) and turbidite (tentatively most distal). They all interfinger throughout the section. In certain intervals of the section, particular facies associations occur more frequently than others, which we generalize into facies units. Five types of facies units may be distinguished based on the frequency of occurrence of its constituent facies associations: (*i*) delta top and shallow delta in comparable proportion; (*ii*) prevalent shallow delta; (*iii*) shallow delta and lake-dominated in comparable proportion; (*iv*) prevalent lake-dominated offshore;

**Table 1**
Sedimentary features of facies associations.

| Facies association | Sedimentary features (in order of significance) | | Thickness (m) |
|---|---|---|---|
| | in sandstones/sands | in muds | |
| Lake-dominated (shoreface, offshore) | shell-rich, erosive surfaces, structureless, superficially reddish, trace fossils, graded bedding | shell-rich layers, scattered mollusk shells, structureless, superficially reddish layers, monotonous gray, parallel lamination | 0.1–70 |
| Shallow delta (delta front, prodelta) | parallel bedding, meter-scale cross-bedding, current cross-lamination, parallel lamination, wave ripples, load structures, convolute bedding, decimeter-scale cross-bedding, minor erosive surfaces, rare mollusk shells | parallel lamination, fissility, monotonous gray-brown, superficially reddish layers, rare mollusk shells | 2–10 |
| Turbidite (hyperpycnite?) | crude parallel bedding, structureless, erosive surfaces, scattered mollusk shells | (the same as in shallow delta muds above) | 1–10 |
| Delta top (channel, crevasse splay, levee, floodplain) | thick (irregular) bedding, crude parallel bedding, erosive surfaces, decimeter-scale cross-bedding, parallel lamination, current cross-lamination, convolute bedding, mud and coal clasts, gray-orange mottling, rare mollusk shells | gray-orange mottling, structureless, coaly mud layers, coal layers, greenish-gray, rare mollusk shells | 0.1–50 |

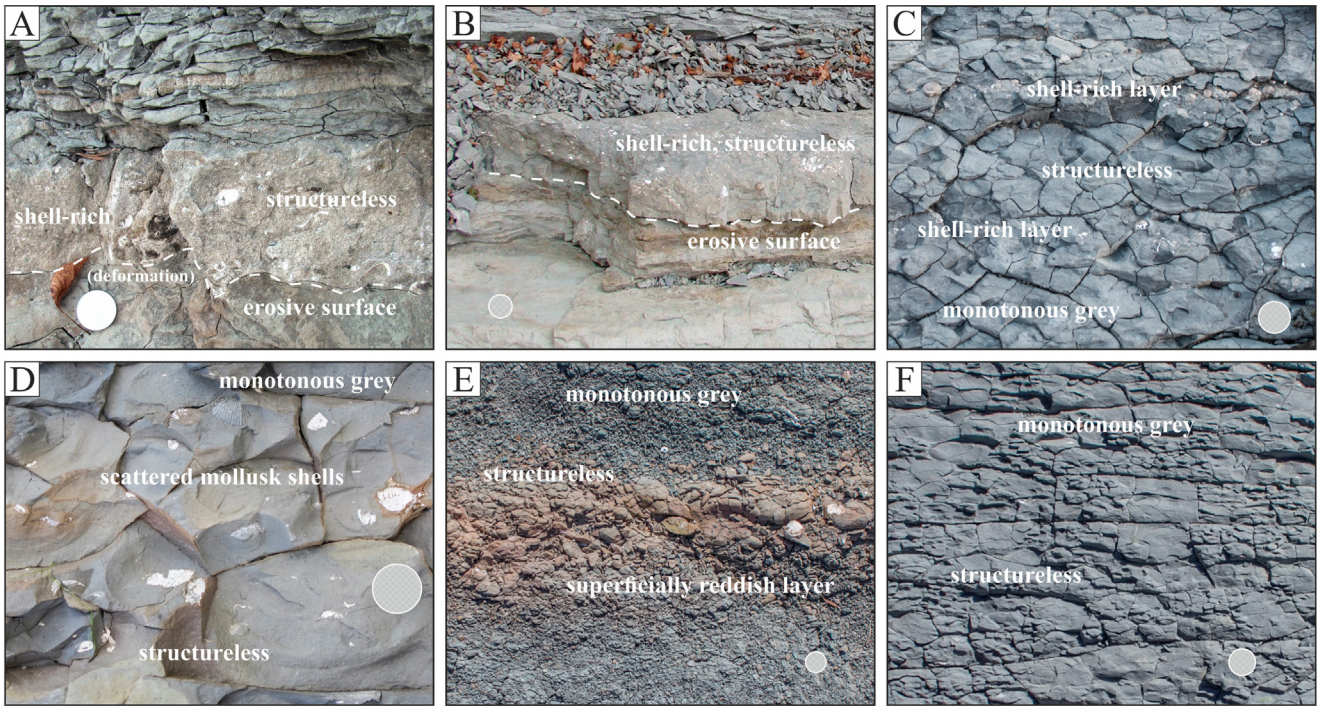


**Fig. 11.** Common features of the lake-dominated facies association. **A, B**. Typical thin sandstones (shoreface) interfingering with shallow delta facies association. **C-F**. Typical muds (offshore).

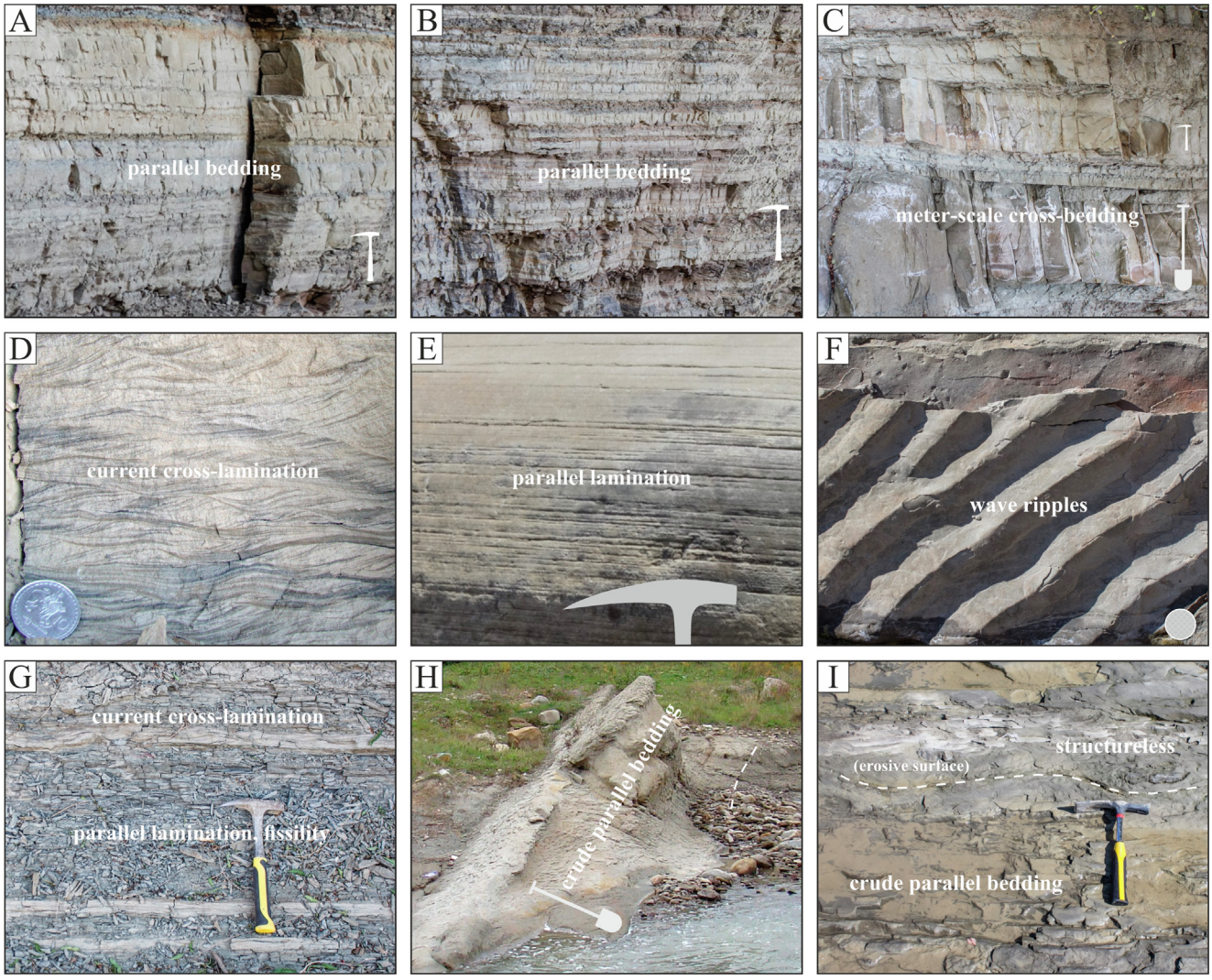


**Fig. 12.** Common features of the shallow delta (delta front, prodelta) and turbidite facies associations. **A-F**. Typical sandstones (delta front). **G**. Typical muds (prodelta). **H, I**. Typical sandstones of turbidite facies association.

(*v*) lake-dominated offshore and secondary turbidite. These types of facies units are particularly useful to visualize large-scale changes in depositional environment along the section (Fig. 14).

## 5. Discussion

The presented ostracod, mollusk and paleomagnetic records as well as age estimates are largely in agreement with previous stratigraphic studies (see Section 2.1), but integrated with the sedimentology and illustrated in greater detail (Figs. 2, 14). The position of the Dacian Basin Pontian stage and its substage boundaries in the section are revised where necessary, according to their biostratigraphic definitions (Marinescu and Papaianopol, 1989). The new dataset is compared with previous results in the adjacent Slănicul de Buzău record of the Dacian stage (Jorissen et al., 2018) and previous results in the nearby Râmnicu Sărat section, covering the whole Pontian (Stoica et al., 2013). We also highlight some new insight that our work offers on the correlation of sedimentary trends, potential local limitations to chronostratigraphy and restriction of the Dacian Basin during the Pontian.

### 5.1. Integrated stratigraphy

The Pontian comprises a ~1780 m thick interval in the Slănicul de Buzău section. It is underlain by the Maeotian (Lazarev et al., 2020) and overlain by the Dacian (Jorissen et al., 2018).

The upper part of the Maeotian is characterized by parasequences of a shallow delta alternating with lake-dominated facies in comparable proportion (facies unit type 3, ~20–65 m interval; Fig. 14). The mollusks show relatively short-lasting monospecific assemblages, while the ostracods are dominated by euryhaline species with low diversity. The fauna is mainly indicative of a stressed brackish-water environment unfavorable for species richness.

There is a thin interval (65–75 m) with foraminifera (Fig. 10) that occur in offshore muds interbedded with thin sandstones rich in *Coelogonia pseudorostriformis* and possibly delta top muds in the lower part. The foraminifera assemblage is dominated by benthic mesohaline to polihaline foraminifera like *Ammonia beccarii*, *Ammotium* sp., *Quinqueloculina akneriana*, *Q. gracilis*, *Prosononion* sp. and the planktonic species *Streptochilus* sp. indicative of stressed conditions (Stoica et al., 2013). The *Coelogonia pseudorostriformis* shells are probably transported from slightly shal-

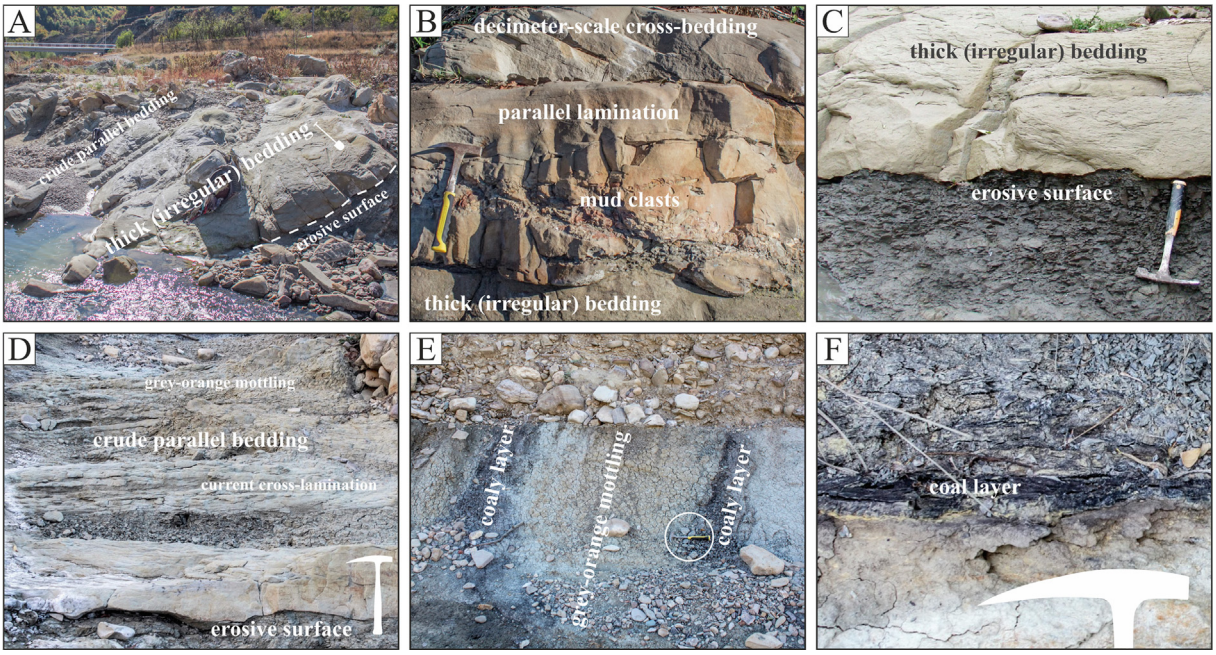


**Fig. 13.** Common features of the delta top facies association. **A-D**. Typical sandstones (channel, crevasse splay, levee). **E, F**. Typical muds (floodplain).

lower areas nearby. The interval with foraminifera and *Coelogonia pseudorostriformis* is usually attributed to the uppermost Maeotian in the Eastern Paratethys (Krijgsman et al., 2010; Stoica et al., 2013; Popov et al., 2016). However, Lazarev et al. (2020), who studied the Maeotian interval of Slănicul de Buzău, reasoned that it was more logical to place the base-Pontian at the first occurrence of these foraminifera. We prefer to attribute the foraminifera to the uppermost Maeotian, in line with the majority of preceding studies and the biostratigraphic definition of the Pontian. The uppermost Maeotian interval has a normal magnetic polarity correlated to chron C3An.1n and a 1.26 m/kyr average sedimentation rate.

It is overlain by an interval mainly represented by lake-dominated offshore facies including possible minor turbidite and shallow delta facies in its lower and upper parts respectively (facies unit type 4, ~75–330 m interval; Fig. 14). The Odessian turnover of mollusks and ostracods occurs at the ~80 m level, slightly postdating the facies change and the foraminifera interval (Figs. 7, 10). The Odessian-Portaferrian boundary is located at ~160 m in the section and is marked by the appearance of both mollusk and ostracod marker species. There is, on the other hand, no clear change in sedimentary facies at this level. The sedimentary interpretation is confirmed by the overall abundance of brackish-water fauna. In addition, the mollusks and ostracods indicate progressive drowning from a deep littoral to deep profundal environment, while the minor shallow delta facies in the upper part (~250 m level) indicate a short water-level fluctuation. The Odessian-Portaferrian boundary coincides with the switch from normal to reversed polarity at the top of the C3An.1n chron. The succeeding chron C3r continues with a 1.32 m/kyr average sedimentation rate.

These distal environments then rapidly switch to much more proximal ones as evident from sedimentary facies, mollusk and ostracod assemblages. We note that this apparent switch in lithology is also commonly inferred to represent the Odessian-Portaferrian boundary in Romanian maps and literature (Vasiliev et al., 2004; Stoica et al., 2013), but it clearly occurs at a younger age than the biostratigraphically defined boundary in the Slănicul de Buzău section (see also Section 5.2). The interval overlying the marked transition is characterized by delta top facies and parasequences of a shallow delta facies with minor recurring lake-dominated facies that bear most of the mollusk and ostracod fossils present in this interval (facies unit type 1, ~330–755 m interval; Fig. 14). The notable facies trend is an overall decrease in delta top facies upwards, which are replaced mainly by shallow delta facies. The fauna is indicative of freshening and shallowing of the lake-dominated environment and synchronous with the regressive facies shift, as manifested in the low diversity of the ostracods and relatively high diversity of the mollusks, which include freshwater and euryhaline taxa. The many barren microfauna samples indicate that much of the mud present in this interval did not accumulate in a lake-dominated (offshore) environment, but rather as floodplain or prodelta facies. The interval continues into chron C3r and is consequently estimated to have deposited at the same 1.32 m/kyr average sedimentation rate calculated over this chron.

The overlying Bosphorian interval (~735–1860 m interval; Fig. 14) is characterized by a clear vertical differentiation of facies. Its beginning slightly predates (~20 m) a rapid flooding establishing turbidite deposition, probably the most distal environment present in the Pontian of Slănicul de Buzău, along with prevalent lake-dominated offshore facies (unit type 5, ~755–850 m interval). It is overlain by lake-dominated facies interfingering on a large-scale with stacked parasequences of shallow delta facies and on a small-scale delimiting individual parasequences (unit type 3, ~850–1030 m interval). The proportion of shallow delta facies increases upwards, indicating a gradual regression.

These two facies units bear abundant brackish-water fauna with many species known from the Odessian as well as some species that newly appeared (Figs. 7, 10). The appearance of brackish-water ostracods at the base of Bosphorian slightly postdates the mollusk turnover and is associated with the interpreted rapid flooding. Despite fairly high-resolution sampling, foraminifera were never found at this level. The mollusks are indicative of fluctuating environments shallowing upwards as a whole from deep profundal to littoral (Fig. 7). Mollusk assemblages generally follow the interpreted facies pattern. It should furthermore be noted that the mollusk assemblages that occur in the continuous offshore

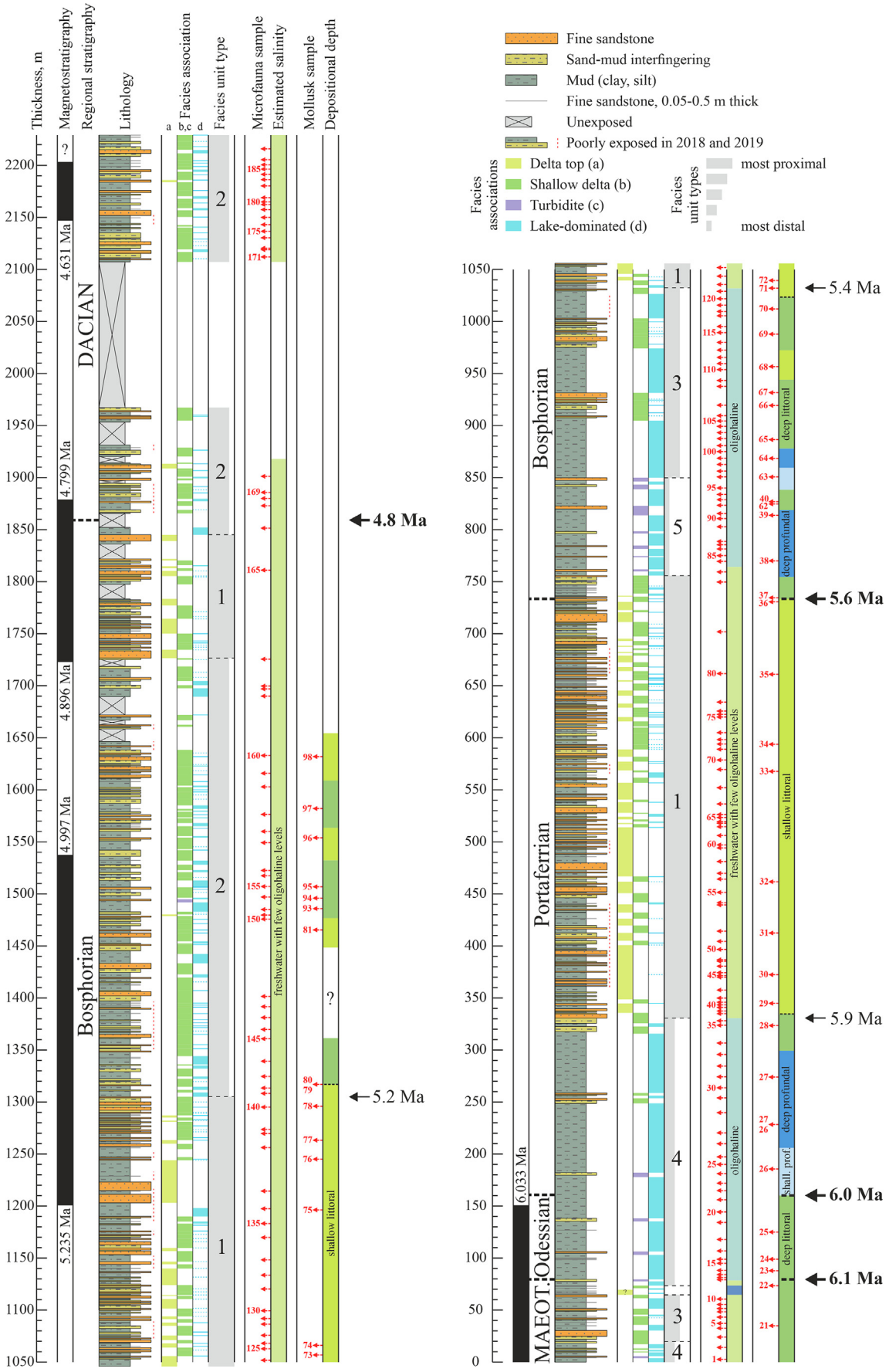


**Fig. 14.** Log of the investigated interval of the Slănicul de Buzău section with correlated sedimentary facies and fauna records as well as magnetostratigraphy, biostratigraphy and estimated age of the main events. See Figs. 3, 7, 10 for paleomagnetic, mollusk (depositional depth) and microfauna (estimated salinity) details, respectively.

muds are very similar to those occurring in thin lake-dominated intervals in the parasequences in the upper part of this interval (facies unit type 3). This indicates that salinity was similar in more distal and more proximal environments with stagnant water. It highlights that when changes in the mollusk fauna do occur in other parts of the section, variations in delta proximity and water-depth may not be the driving mechanism, but other factors, such as basin-wide salinity changes and migrations, may exert greater control.

The regressive trend eventually leads to the deposition of a proximal facies unit characterized by delta top facies and parasequences of a shallow delta facies with a minor lake-dominated facies (unit type 1, ~1030–1305 m interval). Similarly to the Portaferrian, ostracods become relatively scarce and the ostracod and mollusk assemblages change affinity to a freshwater shallow littoral environment, albeit with some brackish-water fluctuations. Chron C3r continues up to the middle of this facies unit. Its upper part falls in chron C3n.4n in which the average sedimentation rate increases to 1.42 m/kyr.

A subsequent minor transgressive shift leads to the establishment of the prevalent parasequences of a shallow delta facies with a secondary contribution of lake-dominated facies (unit type 2) in the ~1305–1725 m interval. This interval furthermore shows subtle changes in fauna indicative of a fluctuating environment, ranging from fresh- to brackish-water and from shallow to deep littoral. While the lower resolution paleontological sampling precludes a full view of the paleoenvironmental fluctuations in the upper part of Bosphorian, the high ostracod abundance and diversity in the 1470–1530 m interval indicates a period with a more stable-brackish water influence, which is not revealed in the relatively impoverished samples above this level. The facies unit continues in chron C3n.4n and passes into chron C3n.3r.

The uppermost Bosphorian shows fragmentary exposure and is characterized by appearance of a noticeable delta top facies component, which suggests a slight regression (unit type 1, ~1725–1845 m interval). There is very limited fauna data from this interval. Its beginning roughly coincides with the boundary between chrons C3n.3r and C3n.3n. Together these two short chrons suggest an increased 1.72 m/kyr average sedimentation rate.

The overlying Dacian unit returns to prevalent parasequences of a shallow delta facies with secondary lake-dominated facies (unit type 2, ~1845–2230 m interval; Fig. 14), but a large part in the middle of this interval is unexposed. While the Pontian and Dacian are biostratigraphically defined, there is a very gradual change in mollusk assemblage at the transition, and the change in ostracods is even more subtle (see also Section 5.3). The beginning of the Dacian roughly coincides with the boundary between chrons C3n.3n and C3n.2r. The latter continues to the upper part with a 1.60 m/kyr average sedimentation rate and is overlain by chron C3n.2n. Similar results were found in the Dacian of the middle segment of the Slănicul de Buzău section (Jorissen et al., 2018).

The ages of the stratigraphic boundaries are calculated assuming constant sedimentation rates between the observed paleomagnetic reversals. It should be noted that this disregards likely changes in sedimentation rate associated with major shifts in depositional environment, but it is the best approach currently available. The Pontian at Slănicul de Buzău is dated between ~6.1 Ma and ~4.8 Ma (Figs. 2, 14) and thus lasted ~1.3 myr. The Odessian lasted from ~6.1 to ~6.0 Ma. The subsequent Portaferrian lasted from ~6.0 to ~5.6 Ma, with a marked switch to a more proximal paleoenvironment at 5.9 Ma. The Bosphorian lasted from ~5.6 to ~4.8 Ma with the initial Bosphorian highstand from ~5.6 to ~5.4 Ma, lower water levels from 5.4 Ma, followed by a second, but less prominent flooding at ~5.2 Ma. Environments are difficult to interpret at the Pontian-Dacian transition due to limited outcrop. In addition, the exact timing of regressive events may be affected by the local setting, which will be discussed in more detail in Section 5.4.

### 5.2. Biostratigraphic definition of the Odessian and Portaferrian boundary

In comparison with the Râmnicu Sărat section, fossils are more abundant along the Slănicul de Buzău section, which is explained by its slightly more distal position in the depositional system. While the content of microfossils and mollusks is in good agreement between the sections, Slănicul de Buzău allows a more detailed biostratigraphic and paleoenvironmental evaluation.

One important change in the stratigraphic approach in comparison with previous studies (e.g., Krijgsman et al. 2010; Lazarev et al., 2020) is that we here apply the biostratigraphic definition of the Dacian Basin Pontian stage given by Marinescu and Papaianopol (1989). In line with that definition, we shift the Odessian (Pontian) lower boundary slightly upwards, to the first occurrence of *Pseudoprosodacna* in the section, whereas it was previously placed at the influx of marine foraminifera (Lazarev et al., 2020). Moreover, we tie the base of the Portaferrian to the first occurrence of *Congeria* (*Rhombocongeria*) *rhomboidea*, whereas previously it was placed 150 m above at the major shift to more sand-rich proximal environments and impoverished faunas, in line with Romanian geological maps (Stoica et al., 2007, 2013; Krijgsman et al 2010; van Baak et al 2017). The latter is known as the Portaferrian or middle Pontian regression and is habitually used to divide the Pontian into a lower, middle and upper lithostratigraphic unit throughout the Dacian Basin.

This change in approach clearly increases the age of the Odessian/Portaferrian boundary, but does not impact the stratigraphic position of the major Portaferrian drawdown, which is equally well expressed at Slănicul de Buzău and Râmnicu Sărat (Fig. 2). Note that the first occurrence of *Congeria* (*Rhombocongeria*) *rhomboidea* in the Dacian Basin reflects the moment of its immigration from Lake Pannon, where it was present since ~8 Ma (Magyar, 2021). The absence of deeper water sublittoral conditions in the Slănicul de Buzău during the Odessian, required by this species (Magyar, 2021), could have created an ecological barrier, preventing its earlier appearance.

Whether one favors a biostratigraphic or base-level related stratigraphic subdivision of the Pontian probably depends on the data at hand, as well as simple personal preference. We have here chosen for a biostratigraphic approach rooted into the paleontological literature of the region.

### 5.3. Bosphorian-Dacian transition in the context of previous results

Because of poor outcrop conditions, the uppermost Bosphorian was not sampled for mollusks. The present study thus only allows indirect evaluation of the Pontian-Dacian transition. To this end, we compare the assemblage of the here-investigated part of the upper Bosphorian with the lower Dacian mollusk record from segment 2 of the Slănicul de Buzău section (Fig. 1(C)) recently published by Jorissen et al. (2018). We follow the original definition of the Dacian stage by Marinescu and Papaianopol (1995).

As we noted above, some representatives of the genera *Stylodacna* and *Pachyprionopleura*, which diversify in the Dacian, are already present in the uppermost samples of the studied Pontian interval. The subsequent onset of the Dacian is marked by the first occurrence of several species such as *Prosodacna obovata*, *Parapachydacna serena*, *Pseudocatillus dacianus* and *Euxinicardium olivetum*, and establishment of slightly deeper water conditions. Whereas *Prosodacna obovata* is also known from the Black Sea Basin, where it is restricted to the lower Kimmerian, the other three taxa are endemic to the Dacian Basin. *Stylodacna heberti* is

also present in the lowermost Dacian interval, whereas *Pachyprionopleura* is recorded somewhat higher up in the lower Dacian (Jorissen et al., 2018).

*Pachyprionopleura* moreover is one of the taxa that becomes very prominent in the Dacian of the Dacian Basin, where it diversifies into 12 species (Papaianopol, 1984, 1995). In the Black Sea Basin, on the other hand, the genus *Pachyprionopleura* only includes *P. moquicum*, which is characteristic for the Kimmerian stage. This reflects the increasing biogeographic separation of the Dacian Basin and the Black Sea in the latest Bosphorian/early Kimmerian (Nevesskaja et al., 1997, 2001).

Judging from the overwhelming number of endemic species, the Dacian bivalve record was gradually enriched through autochthonous speciation due to the restricted paleogeographic setting of the Dacian Basin and low extinction rates due to stable environmental conditions, which resulted in species accumulation (Papaianopol, 1995; Nevesskaja et al., 2001; Jorissen et al., 2018). The short-term Pliocene increase in global temperatures, which interrupted the global cooling trend set in motion by the Miocene Climate Transition (Herbert et al., 2016), may also have been beneficial to this spectacular endemic mollusk diversification. The gradual shift in the faunal composition makes it difficult to pinpoint the Pontian/Dacian boundary, in line with the observation of Stoica et al. (2007). The same holds true for the Black Sea Basin where the upper Pontian and Kimmerian mollusk faunas are closely related in the absence of any major extinction events (Nevesskaja et al., 1986, 2001).

### 5.4. Local constraints of the chronostratigraphy

As the Slănicul de Buzău record represents insight into the paleoenvironmental evolution at one point in space, several factors may decrease its utility for chronostratigraphic correlation. Local factors, such as subsidence, sediment supply and depth, may contribute to and obscure environmental and faunal responses to regional changes in water-level, fauna migrations or evolution. A strong depth-sensitivity of index species was particularly noted for the neighboring Lake Pannon, where progradation of major clinoforms was routinely mistaken for basin-wide stratigraphic change (Magyar, 2021).

It is important for the interpretation of the Slănicul de Buzău record that major clinoforms had prograded across the Focşani depression by the end of the early Maeotian and since then deposition occurred mainly within shallow-water and fluvial environments of seismic topsets, i.e., deposition occurred on the shelf (Krézsek and Olariu, 2021). Our record confirms prevalence of such environments during the studied period. However, we can expect that the Odessian–lower Portaferrian and lower Bosphorian transgressive intervals were likely associated with drowning and subsequent progradation of modest (sub-seismic) clinoforms that could noticeably influence fauna composition. As the three-partite Pontian biostratigraphy is recognized in many locations in the Eastern Paratethys (Stevanović et al., 1989), local factors did not obscure the main Pontian trends in the Slănicul de Buzău section. However, the precise timing of the identified biostratigraphic boundaries may have been influenced by the site-specific balance of sediment supply, subsidence and lake-level, as well as salinity.

A cyclic littoral deposition associated with the identified Maeotian-Pontian boundary was likely to allow rapid colonization by new species in response to a striking fauna migration at ~6.1 Ma, making this biostratigraphic boundary very well suited for chronostratigraphy. The following Odessian–Portaferrian boundary is a clear example where the choice of criteria for its definition can significantly affect its chronostratigraphic position. The presently used appearance of several index species at this boundary, dated at ~6.0 Ma, is associated with a mild deepening trend that could have delayed local appearance of depth-sensitive species. However, the rapid appearance of several new species at the background of a gradual environmental trend suggests that an immediate registration of fauna migration is more likely. The alternative definition of this boundary follows the marked environmental shallowing driven by a water-level drop in Portaferrian (Popov et al., 2010), which onset should have been diachronous throughout the basin, depending on local progradation rates. Such diachrony is evident in the Western Dacian Basin from the progradation of seismic scale clinoforms at this time (Leever et al., 2010; Krézsek and Olariu, 2021). While the rapid shallowing occurs notably later (at ~5.9 Ma) than the appearance of index species in the here-studied record, such a delay could have been caused by the high subsidence rate at Slănicul de Buzău.

The Portaferrian-Bosphorian boundary is associated primarily with the onset of rapid environmental deepening driven by a water-level rise (Popov et al., 2010), leading to a massive turnover of depth-sensitive species as well as the appearance of some new species at ~5.6 Ma. This change was unlikely to be delayed at the background of flat shelf-top coastal deposition in the Slănicul de Buzău section. However, since this boundary is recognized through marked environmental deepening its distinguishability may significantly decrease in deeper environments. The subsequent gradual progradation, leading to maximum shallowing between ~5.4 and ~5.2 Ma, could have been somewhat delayed due to the high subsidence rate at Slănicul de Buzău, similarly to the Portaferrian. Finally, the uneventful cyclic littoral deposition in the Slănicul de Buzău section was unlikely to obscure a gradual change in fauna across the Pontian-Dacian boundary driven by evolution, while the boundary's position is still inherently imprecise.

### 5.5. Comparison with the Râmnicu Sărat record

The present analysis was conducted to improve a previously published stratigraphic record for the Pontian of the Dacian Basin from the neighboring Râmnicu Sărat section (Vasiliev et al., 2004; Krijgsman et al., 2010; Stoica et al., 2013). The main drawback of the Râmnicu Sărat record is the fragmentary exposure of the Pontian, leading to a lower resolution of sampling and a less accurate thickness (and thus age) model.

Particularly important is that along Râmnicu Sărat, there are poor exposures at the Maeotian-Pontian boundary, which means that the position of the reversal at the base of C3r is determined by a single reversed sample followed by a 100 m gap in the magnetostratigraphic record. This is particularly cumbersome considering the complexity of the interpretation of the paleomagnetic signal near the base of the Pontian, where our high-resolution analysis reveals frequently alternating polarities (Fig. 3). The base of the C3r chron may therefore either be placed in the Odessian, if one interprets an early diagenetic down-working reverse overprint, or in the uppermost Maeotian, if one prefers a high-temperature overprint with normal directions in tectonic coordinates. We consider the first option more likely. This does imply that the base of the C3r chron shifts upwards with respect to the biostratigraphic Maeotian-Pontian boundary in comparison with previous studies. In order to obtain higher-resolution (<100 kyr) chronological constraints on the events in the Maeotian-Pontian boundary interval, which is beyond the scope of this study, a detailed rock-magnetic study should be carried out in order to understand the origin and significance of the two components. In any case, our study reveals that care should be taken with the interpretation of paleomagnetic directions near the base of the Pontian, in particular when sampling density is as low as along the Râmnicu Sărat section.

All the estimated ages from the two sections are within the plausible ± 0.1 Ma error margin with exception of the revised Odessian-Portaferrian boundary (Fig. 2). The general problem affecting both sections is likely the significant variation of sedimentation rate during the long C3r chron covering the Portaferrian and lower part of the Bosphorian. The sedimentation rate in this interval is expected to be locally affected by significant changes in both depositional depth and base level. A better exposure and abundance of fauna in the Slănicul de Buzău section makes it a preferred stratigraphic record with higher potential for future improvement such as astronomical tuning.

### 5.6. Correlation of sedimentary trends

The short marine incursion at the Maeotian-Pontian transition (~6.1 Ma), reflected in the occurrence of foraminifera, is often considered as evidence of a marine flooding in the Eastern Paratethys that rapidly led to more distal depositional environments (Krijgsman et al., 2010; Stoica et al., 2013; Lazarev et al., 2020). Our facies record shows a shallowing period in the latest Maeotian, immediately followed by the influx of foraminifera (~10 m thick interval), but the environmental deepening was by contrast significantly protracted, marked both by a slowly increasing proportion of mud and by a changing faunal composition upwards (~75–230 m interval; Figs. 7, 14). In particular, our data indicate that the moment of marine connectivity preceded the water-level highstand in the Dacian Basin by roughly 100–150 kyr. Moreover, the conditions for intermittent marine connectivity in the Eastern Paratethys could have been established even earlier in the late Maeotian, as evidenced by a sample with marine foraminifera in the studied section (Lazarev et al., 2020) and occasional marine nannofossils in the long preceding interval (6.4–6.1 Ma) in the NE Black Sea (Radionova and Golovina, 2011).

While distal facies of the upper Maeotian suggests that a larger scale base-level rise could have also started earlier (Lazarev et al., 2020), the first major turnover of fauna occurred in the early Odessian, followed by the arrival of another set of immigrant taxa at the onset of the Portaferrian. These events introduced many new species from the mesohaline Lake Pannon and were associated with a widespread transgression in the Eastern Paratethys (see Section 2.1). The Odessian highstand, presently identified as Odessian-early Portaferrian, was shown to be unrelated to eustacy suggesting a need for an alternative explanation (Popov et al., 2010). In a landlocked basin, like the Eastern Paratethys, it can be achieved through a tectonic uplift of an overflowing gateway, which in this case was probably directed to the Mediterranean through the Aegean (Krijgsman et al., 2020).

Our faunal record indicates that the environment at Slănicul de Buzău became even deeper in the lower part of the Portaferrian than during the Odessian. This is a little puzzling: In the nearby low-accommodation Odessa region along the northern coast of the Black Sea, deposits with Odessian fauna, which accumulated as a result of the prominent transgression of the coast, are plentiful and very well-known (Stevanović et al., 1989). However, no overlying Portaferrian deposits (i.e., with the *Congeria* (*Rhombocongeria*) and *Caladacna* species) have ever been identified in that region. This may be explained by the marked difference in subsidence rates between the Focşani Depression and the northern coast of the Black Sea which may have delayed maximum flooding at Slănicul de Buzău.

Our facies record of the sand-dominated part of the Portaferrian shows progradation with at least occasional minor transgressions that became more common in the upper part (Fig. 14). Together with the considerable thickness of deposits (~405 m), this implies an overall moderate base-level drop in the Dacian Basin, largely compensated by fast subsidence in the investigated Focşani Depression. In fact, the Portaferrian is associated with a much lower amplitude base-level drop (~100 m) in the western Dacian Basin (LST2 unit in Leever et al., 2010; Krézsek and Olariu, 2021) than in the Black Sea basin where it reaches ~500 m (Popov et al., 2010; Krézsek et al., 2016; Fig. 2). It is possible that the base-level fall in the Dacian Basin was limited by the gateway towards the Black Sea in combination with a positive water balance, which is also implied by horizontal shelf-edge trajectories visible on seismic sections (Leever et al., 2010; Munteanu et al., 2012; Fongngern et al., 2016) and strontium isotope ratios that indicate a predominance of local river water in the Dacian Basin (Vasiliev et al., 2021). For the Black Sea, on the other hand, highly evaporative conditions are inferred from deuterium indicators at this time (Vasiliev et al., 2013, 2015), suggesting a negative water balance in analogy with the Mediterranean, although import of deuterium-enriched water from the Mediterranean through atmospheric circulation and precipitation cannot be ruled out.

The Portaferrian-Bosphorian turnover (~5.6 Ma) at present seems the only good chronostratigraphic correlative with events of the Messinian Salinity Crisis in the Mediterranean (Fig. 2). It matches reasonably well with the 5.55 Ma onset of the Lago-Mare stage (Roveri et al., 2014). Progressively similar environments and probably increased water flux towards the Mediterranean basin is evidenced by the remarkable migration of the brackish Paratethyan fauna to the Mediterranean during this interval (Roveri et al., 2014; Stoica et al., 2016; Grothe et al., 2018; Andreetto et al., 2021, 2022). The near coincidence with the 5.5 Ma major deglaciation (Hodell et al., 2001) suggests that a change of the regional climate may have caused an increased input of continental water, raising the base-level in the Eastern Paratethys and leading to overflow towards the Mediterranean. The rapidity of the turnover in the studied section may point towards a rapid shift in climate setting.

Local sequence stratigraphic correlatives of the initial Bosphorian flooding are the TST2 sequence in the Dacian Basin (Leever et al., 2010) and the upper part of the SQ3 sequence in the Black Sea (Munteanu et al., 2012) (Fig. 2). A lesser height of base-level rise in comparison with the Odessian highstand in the Black Sea could be deduced according to a lack of distinct onshore equivalents, unlike those of the Odessian (Popov et al., 2010). The Mediterranean reestablished full connectivity with the Ocean at the Mio-Pliocene transition (5.33 Ma), while there are shallowing and freshening trends in the Slănicul de Buzău section lasting until ~5.2 Ma. This indicates that the rapid marine influx of Atlantic waters, leading to open marine conditions in the Mediterranean, did not reach the Dacian Basin and Eastern Paratethys. At ~5.2 Ma, the sedimentary facies and mollusks of the studied section show a minor transgressive shift, correlating with the onset of the Kimmerian in the Black Sea Basin based on magnetostratigraphy (Popov et al., 2019). However, aside for an intermittent return of the deep-water markers such as *Valenciennius*, an introduction of Kimmerian index fossils has not been recorded in the Slănicul de Buzău section. Instead, the Pontian-Dacian boundary at ~4.8 Ma is represented by a gradual transition in the fauna, which has a strongly endemic character. Coincident with the onset of relative stability of sedimentary environments in the Dacian Basin at 5.2 Ma, there is a major regression in the Caspian Sea leading to deposition of the fluvial Productive Series, which lasted until ~2.95 Ma (Van Baak et al., 2016a; Lazarev et al., 2021; Fig. 2). This suggests major restrictions of connectivity not only with the Mediterranean but also within the Eastern Paratethys after the Mio-Pliocene transition.

### 5.7. Dacian Basin restriction

The apparent divergence of the mollusk faunas of the Dacian and Black Sea basins even during transgression implies a continuous connectivity restriction (Nevesskaja et al., 1986). This is confirmed by a lasting difference in strontium isotope ratios between the Black Sea and Dacian Basin for the studied period (Vasiliev et al., 2021). An explanation for this can be offered based on the geological setting of the likely gateway area (Fig. 1(A)). The gateway location to the north of Dobrogea was suggested paleogeographically (Popov et al., 2004; Jipa and Olariu, 2009) and substantiated by subsurface data (Matoshko et al., 2009, 2019). These subsurface data furthermore revealed that deposition continued during the Pontian, suggesting restriction was not due to uplift of the gateway area. It was recognized that progradation of the East Carpathian foreland axial drainage system probably resulted in sediment supply to both the Dacian Basin and the Black Sea (Matoshko et al., 2016; de Leeuw et al., 2020), diverging in front of Dobrogea. An analysis of seismic sections furthermore indicates that the East Carpathian foreland axial drainage system prograded markedly into the Black Sea during the Bosphorian (de Leeuw et al., 2020).

A potential mechanism for the restriction of the gateway between the Black Sea and the Dacian Basin is that sediment supplied by the East Carpathian Foreland axial fluvio-deltaic system clogged the passage and to some degree counteracted its enlargement during a base-level rise. The apparent importance of the regional continental water influx in the Dacian Basin distinct from the Black Sea according to strontium isotope ratios (Vasiliev et al., 2021) implies a prevailing outflow towards the latter. This means that stabilization of a relatively freshwater environment in the Dacian Lake, at least in the upper part of its water column, is to be expected in the absence of backflow from the higher salinity Black Sea. Such conditions would have been even more likely if the level of the Black Sea dropped below the gateway, preventing even occasional backflow. This situation could, on the other hand, have only lasted for a short time before incision would have ground away the sill between the basins, thus equalizing their levels.

The comparison between mollusk and ostracod fauna and facies changes shows rather a trend correlation than direct correspondence because facies variability cannot explain all noticeable changes in fauna. It is possible that the water-level modulated both the local depth and gateway permeability, affecting the local facies and basin-wide fauna correspondingly with a similar timing. The basin-wide changes to fauna ecology could have occurred synergically with local freshwater input by the delta, reducing salinity during base-level fall and increasing salinity during base-level rise.

## 6. Conclusion

We present an integrated stratigraphic record of paleomagnetism, mollusks, microfossils and sedimentary facies covering the Pontian regional (Eastern Paratethys) stage according to its historical definition in the Dacian Basin. This record contributes to similar previous results with improved resolution and completeness. As the ages are linearly interpolated between the paleomagnetic reversals, their accuracy is affected by local changes of sedimentation rate, which are expected to be significant.

The Odessian interval (lower Pontian) begins with a transgressive shift in facies and the appearance of many new brackish-water species dated at 6.1 Ma. The Odessian-Portaferrian boundary is here pinpointed by the first occurrence of several characteristic mollusk and ostracod species within a distal facies and brackish-water environment at 6.0 Ma. It is followed at 5.9 Ma by a prominent regression resulting in predominant delta-top deposition and a switch to freshwater fauna. This persisted throughout the Portaferrian interval (middle Pontian), albeit with a return of some delta-front deposition, until 5.6–5.5 Ma. The succeeding Bosphorian interval (upper Pontian) began with a rapid flooding and reappearance of many "Odessian–early Portaferrian-type" brackish-water species, as well as the appearance of some new ones. This suggests the Odessian–early Portaferrian species remained present in the deeper parts of the Dacian Basin or the adjacent Black Sea during the Portaferrian lowstand. The Bosphorian transgression was followed by a gradual regression. In the remainder of the Bosphorian, salinities fluctuated between oligohaline and fresh while the sedimentary environment stabilized with distinct but minor fluctuations in relative water level. The first such fluctuation at ~5.2 Ma is marked by a short-term reappearance of deeper water mollusks and might correlate with the Kimmerian (Azovian) transgression in the Black Sea. We place the Bosphorian-Dacian limit at 4.8 Ma, although the position of this boundary is tentative because the faunal change between the Pontian and Dacian occurs gradually and we did not observe a marked change in sedimentary environment either.

The facies record suggests that the Odessian (to early Portaferrian?) highstand in the Eastern Paratethys occurred noticeably later than the marine ingression in the latest Maeotian. Our facies data indicate a moderate base-level drop during the Portaferrian in the Focşani Depression and provides arguments for a subsequent rapid flooding at 5.6–5.5 Ma, coincident with a marked climate change. The subsequent regression and relative stability of sedimentary environments coincided with decreased connectivity with the Black Sea in the Early Pliocene. The main cause of the restriction between the Dacian Basin and the Black Sea is probably the sediment flux from the East Carpathian Foreland axial system which clogged the gateway. Such restriction must have been enhanced or counteracted by respective decreases and increases in base-level. The utility of the stage and substage boundaries described here at Slănicul de Buzău for chronostratigraphic correlation were likely favored, rather than hindered, by the local interplay between subsidence, sediment supply, and lake-level.

## Data availability

Data will be made available on request.

## Declaration of Competing Interest

The authors declare that they have no known competing financial interests or personal relationships that could have appeared to influence the work reported in this paper.

## Acknowledgements

We thank Thomas Neubauer and Imre Magyar for their constructive reviews, which greatly helped to improve the manuscript.

## Appendix A. Supplementary information

Supplementary information (including Table S1) associated with this article can be found, in the online version, at: https://doi.org/10.1016/j.geobios.2023.03.002.

## References

Agalarova, D.A., 1967. Microfauna ponticheskikh otlozhenii Azerbaidzhana i sopredelnykh raionov [Microfauna of the Pontian deposits of Azerbaijan and adjacent regions]. Nedra, Leningrad (in Russian).

Agalarova, D.A., Kadyrova, Z.K., Kulieva, S.A., 1961. Ostrakody pliotsenovykh i postpliotsenovykh otlozhenii Azerbaidzhana [Ostracoda from Pliocene and Post-Pliocene deposits of Azerbaijan]. Azerbaijan State Publisher, Baku (in Russian).
Andreescu, I., 1977. Sistematica lymnocardiidelor prosodacniforme. Subfamilia Prosodacninae 26, 5–74.
Andreetto, F., Aloisi, G., Raad, F., Heida, H., Flecker, R., Agiadi, K., Lofi, J., Blondel, S., Bulian, F., Camerlenghi, A., Caruso, A., Ebner, R., García-Castellanos, D., Gaullier, V., Guibourdenche, L., Gvirtzman, Z., Hoyle, T.M., Meijer, P.T., Moneron, J., Sierro, F.J., Travan, G., Tzevahirtzian, A., Vasiliev, I., Krijgsman, W., 2021. Freshening of the Mediterranean Salt Giant: controversies and certainties around the terminal (Upper Gypsum and Lago-Mare) phases of the Messinian Salinity Crisis. Earth-Science Reviews 216, 103577.
Andreetto, F., Flecker, R., Aloisi, G., Mancini, A.M., Guibourdenche, L., de Villiers, S., Krijgsman, W., 2022. High-amplitude water-level fluctuations at the end of the Mediterranean Messinian Salinity Crisis: implications for gypsum formation, connectivity and global climate. Earth and Planetary Science Letters 595, 117767.
Bertotti, G., Matenco, L., Cloetingh, S., 2003. Vertical movements in and around the south-east Carpathian foredeep: lithospheric memory and stress field control. Terra Nova 15, 299–305.
Bhattacharya, J.P., 2010. Deltas. In: James, N.P., Dalrymple, R.W. (Eds.), Facies models 4. Geological Association of Canada, St John's, pp. 233–264.
Brenchley, P.J., Harper, D.A.T., 1998. Palaeoecology: Ecosystems, Environments and Evolution. Chapman and Hall, London.
Briceag, A., Yanchilina, A., Ryan, W.F., Stoica, M., Melinte-Dobrinescu, M.C., 2019. Late Pleistocene to Holocene paleoenvironmental changes in the NW Black Sea. Journal of Quaternary Science 34, 87–100.
Bridge, J., Demicco, R., 2008. Earth surface processes, landforms and sediment deposits. Cambridge University Press, Cambridge.
Csató, I., Tóth, S., Catuneanu, O., Granjeon, D., 2015. A sequence stratigraphic model for the upper Miocene-Pliocene basin fill of the Pannonian Basin, eastern Hungary. Marine and Petroleum Geology 66, 117–134.
Cziczer, I., Magyar, I., Pipík, R., Böhme, M., Ćorić, S., Bakrač, K., Sütő-Szentai, M., Lantos, M., Babinszki, E., Müller, P., 2009. Life in the sublittoral zone of long-lived Lake Pannon: paleontological analysis of the Upper Miocene Szak Formation, Hungary. International Journal of Earth Sciences 98, 1741–1766.
Danielopol, D.L., Carbonel, P., Colin, J.P. (Eds.), 1990. *Cytherissa* (Ostracoda) – The *Drosophila* of Paleolimnology. Bulletin de l'Institut Géologique du Bassin d'Aquitaine, Bordeaux.
De Leeuw, A., Tulbure, M., Kuiper, K.F., Melinte-Dobrinescu, M.C., Stoica, M., Krijgsman, W., 2018. New 40Ar/39Ar, magnetostratigraphic and biostratigraphic constraints on the termination of the Badenian Salinity Crisis: Indications for tectonic improvement of basin interconnectivity in Southern Europe. Global and Planetary Change 169, 1–15.
De Leeuw, A., Vincent, S., Matoshko, A., Matoshko, A., Stoica, M., Nicoara, I., 2020. Late Miocene sediment delivery from the axial drainage system of the East Carpathian foreland basin to the Black Sea. Geology 48, 761–765.
Dupont-Nivet, G., Vasiliev, I., Langereis, C.G., Krijgsman, W., Panaiotu, C., 2005. Neogene tectonic evolution of the southern and eastern Carpathians constrained by paleomagnetism. Earth and Planetary Science Letters 236, 374–387.
Floroiu, A., Stoica, M., Vasiliev, I., Krijgsman, W., 2011. Maeotian/Pontian ostracods in the Badislava-Topolog area (South Carpathian foredeep, Romania). Geo-Eco-Marina 17, 177–184.
Fongngern, R., Olariu, C., Steel, R.J., Krézsek, C., 2016. Clinoform growth in a Miocene, Para-tethyan deep lake basin: thin topsets, irregular foresets and thick bottomsets. Basin Research 28, 770–795.
Gillet, H., Lericolais, G., Réhault, J.-P., 2007. Messinian event in the black sea: evidence of a Messinian erosional surface. Marine Geology 244, 142–165.
Gliozzi, E., 1999. A late Messinian brackish water ostracod fauna of Paratethyan aspect from Le Vicenne Basin (Abruzzi, central Apennines, Italy). Palaeogeography Palaeoclimatology Palaeoecology 151, 191–208.
Gliozzi, E., Grossi, F., 2004. Ostracode assemblages and palaeoenvironmental evolution of the latest Messinian Lago-Mare event at Perticara (Montefeltro, Northern Apennines, Italy). Revista Española de Micropaleontología 36, 157–169.
Gliozzi, E., Grossi, F., 2008. Late Messinian lago-mare ostracod palaeoecology: a correspondence analysis approach. Palaeogeography Palaeoclimatology Palaeoecology 264, 288–295.
Gliozzi, E., Rodriguez-Lazaro, J., Nachite, D., Martin-Rubio, M., Bekkali, R., 2005. An overview of Neogene brackish leptocytherids from Italy and Spain: biochronological and palaeogeographical implications. Palaeogeography Palaeoclimatology Palaeoecology 225, 283–301.
Gramann, F., Kockel, F., 1969. Das Neogen im Strimonbecken (Griechisch–Ostmazedonien). Teil 1: Lithologie, Stratigraphie und Paläogeographie. Geologisches Jahrbuch 87, 445–484.
Grothe, A., Sangiorgi, F., Brinkhuis, H., Stoica, M., Krijgsman, W., 2018. Migration of the dinoflagellate Galeacysta etrusca and its implications for the Messinian Salinity Crisis. Newsletters on Stratigraphy 51, 73–91.
Hanganu, E., 1974. Observation sur l'ostracofaune pontienne de la région comprise entre la vallée du Danube et la vallée du Motru. Revista Española de Micropaleontología 6, 335–346.
Hanganu, E.N., Papaianopol, I., 1982. Associations significatives du Pontien du Bassin Dacique (Roumanie). Bulletin de la Société belge de Géologie 91, 51–59.
Herbert, T.D., Lawrence, K.T., Tzanova, A., Peterson, L.C., Caballero-Gill, R., Kelly, C.S., 2016. Late Miocene global cooling and the rise of modern ecosystems. Nature Geoscience 9, 843–847.
Hodell, D.A., Curtis, J.H., Sierro, F.J., Raymo, M.E., 2001. Correlation of late Miocene to early Pliocene sequences between the Mediterranean and North Atlantic. Paleoceanography 16, 164–178.
Horne, D., Holmes, J., Rodriguez-Lazaro, J., Viehberg, F. (Eds.), 2012. Ostracoda as Proxies for Quaternary Climate Change. Developments in Quaternary Science 17.
Hsü, K.J., Ryan, W.B.F., Cita, M.B., 1973. Late Miocene desiccation of the Mediterranean. Nature 242, 240–244.
Iljina, L.A., Nevesskaja, L.A., Paramonova, N.P., 1976. Zakonomernosti razvitia molluskov v opresnennykh basseinakh neogena Evrazii [Regularities of mollusk development in the Neogene brackishwater basins of Eurasia (Late Miocene - Early Pliocene)] 155, 1–288 (in Russian).
Jipa, D.C., Olariu, C., 2009. Dacian Basin, Depositional Architecture and Sedimentary History of a Parathetys Sea. Geo-Eco-Marina Special Publication. 3. Geoecomar, Bucharest.
Jorissen, E.L., de Leeuw, A., van Baak, C.G., Mandic, O., Stoica, M., Abels, H.A., Krijgsman, W., 2018. Sedimentary architecture and depositional controls of a Pliocene river-dominated delta in the semi-isolated Dacian Basin, Black Sea. Sedimentary Geology 368, 1–23.
Karanovic, I., 2012. Recent freshwater ostracods of the world: Crustacea, Ostracoda, Podocopida. Springer Science & Business Media, Berlin, Heidelberg.
Karmishina, G.I., 1975. Ostrakody pliotsena yuga evropeiskoi chasti SSSR [Pliocene Ostracods of the Southern European part of the USSR]. Saratov. Gos. Univ., Saratov (in Russian).
Kovács, Á., Balázs, A., Špelić, M., Sztanó, O., 2021. Forced or normal regression signals in a lacustrine basin? Insights from 3D stratigraphic forward modeling in the SW Pannonian Basin. Global and Planetary Change 196, 103376.
Krézsek, C., Olariu, C., 2021. Filling of sedimentary basins and the birth of large rivers: The lower Danube network in the Dacian Basin, Romania. Global and Planetary Change 197, 103391.
Krézsek, C., Schleder, Z., Bega, Z., Ionescu, G., Tari, G., 2016. The Messinian sea-level fall in the western Black Sea: Small or large? Insights from offshore Romania. Petroleum Geoscience 22, 392–399.
Krijgsman, W., Stoica, M., Vasiliev, I., Popov, V.V., 2010. Rise and fall of the Paratethys Sea during the Messinian salinity crisis. Earth and Planetary Science Letters 290, 183–191.
Krijgsman, W., Palcu, D.V., Andreetto, F., Stoica, M., Mandic, O., 2020. Changing seas in the late Miocene Northern Aegean: A Paratethyan approach to Mediterranean basin evolution. Earth-Science Reviews 210, 103386.
Krstic, N., Stancheva, M., 1989. Ostracods of Eastern Serbia and Northern Bulgaria with notices on a Northern Turkey assemblage and some Mediterranean assemblages. In: Stevanovič, P., Nevesskaja, L.A., Marinescu, Fl, Sokač, A., Jámbor, Á. (Eds.), Chronostratigraphie und Neostratotypen: Neogen der Westlichen ("Zentrale") Paratethys 8. Pontien. Jazu and Sanu, Zagreb–Beograd, pp. 753–786.
Larsen, H.C., Saunders, A.D., Clift, P.D., Beget, J., Wei, W., Spezzaferri, S., 1994. Seven million years of glaciation in Greenland. Science 264, 952–955.
Lazarev, S., de Leeuw, A., Stoica, M., Mandic, O., van Baak, C.G.C., Vasiliev, I., Krijgsman, W., 2020. From Khersonian drying to Pontian "flooding": Late Miocene stratigraphy and palaeoenvironmental evolution of the Dacian Basin (Eastern Paratethys). Global and Planetary Change 192, 103224.
Lazarev, S., Kuiper, K.F., Oms, O., Bukhsianidze, M., Vasilyan, D., Jorissen, E.L., Bouwmeester, M.J., Aghayeva, V., Van Amerongen, A.J., Agustí, J., Lordkipanidze, D., Krijgsman, W., 2021. Five-fold expansion of the Caspian Sea in the late Pliocene: New and revised magnetostratigraphic and $^{40}Ar/^{39}Ar$ age constraints on the Akchagylian Stage. Global and Planetary Change 206, 103624.
Leever, K.A., Bertotti, G., Zoetemeijer, R., Matenco, L., Cloetingh, S.A.P.L., 2006. The effects of a lateral variation in lithospheric strength on foredeep evolution: implications for the East Carpathian foredeep. Tectonophysics 421, 251–267.
Leever, K.A., Matenco, L., Rabagia, T., Cloetingh, S., Krijgsman, W., Stoica, M., 2010. Messinian sea level fall in the Dacic Basin (eastern Paratethys): palaeogeographical implications from seismic sequence stratigraphy. Terra Nova 22, 12–17.
Livental, V.E., 1929. Ostracoda akchagylskogo i apsheronskogo yarusov po Babazanskomu razrezu [Ostracoda of Akchagilian and Apsheronian beds of the Babazan section] 1, 1–58 (in Russian).
Lubenescu, V., Zazuleac, D., 1985. Les Viviparidés du Néogène supérieur du Bassin Dacique 32, 77–136.
Macalet, R., 2002. Nouvelles espèces du genres *Zagrabica* et *Melanoides* dans le Dacien du bassin Dacique. Acta Paleontologica Romaniae 3, 257–265.
Magyar, I., 2021. Chronostratigraphy of clinothem-filled non-marine basins: Dating the Pannonian Stage. Global and Planetary Change 205, 103609.
Magyar, I., Radivojević, D., Sztanó, O., Synak, R., Ujszászi, K., Pócsik, M., 2013. Progradation of the paleo-Danube shelf margin across the Pannonian Basin during the late Miocene and early Pliocene. Global and Planetary Change 103, 168–173.
Mandelstam, M.I., Schneider, G.F., 1963. Iskopaemye ostracody SSSR. Semejstvo *Cyprididae* [Fossil ostracods of the USSR. Family *Cyprididae*]. Trudy VNIGRI, Leningrad [in Russian].
Marinescu, F., 1977. Genre *Dreissenomya* Fuchs (Bivalven, Heterodonta) 26, 75–118.
Marinescu, F., Papaianopol, I., 1989. Le Pontien du Bassin Dacique en Roumanie. In: Stevanović, P., Nevesskaja, L.A., Marinescu, F., Sokač, A., Jambor, Á. (Eds.),

Chronostratigraphie und Neostratotypen: Neogen der Westlichen (“Zentrale”) Paratethys 8. Pontien. Jazu-Sanu, Zagreb-Beograd, pp. 300–313.
Marinescu, F., Papaianopol, I. (Eds.), 1995. Pliozän Pl1, Dacien. Chronostratigraphie und Neostratotypen: Neogen der Zentralen Paratethys 9. Editura Academiei Romane, Bucuresti.
Marzocchi, A., Flecker, R., Van Baak, C.G.C., Lunt, D.J., Krijgsman, W., 2016. Mediterranean outflow pump: an alternative mechanism for the Lago-mare and the end of the Messinian salinity crisis. Geology 44, 1–4.
Matenco, L., Bertotti, G., Leever, K., Cloetingh, S.A.P.L., Schmid, S.M., Tărăpoancă, M., Dinu, C., 2007. Large-scale deformation in a locked collisional boundary: Interplay between subsidence and uplift, intraplate stress, and inherited lithospheric structure in the late stage of the SE Carpathians evolution. Tectonics 26, TC4011.
Matoshko, A.V., Gozhik, P.F., Semenenko, V.N., 2009. Late Cenozoic fluvial development within the Sea of Azov and Black Sea coastal plains. Global and Planetary Change 68, 270–287.
Matoshko, A., Matoshko, A., de Leeuw, A., Stoica, M., 2016. Facies analysis of the Balta Formation: Evidence for a large late Miocene fluviodeltaic system in the East Carpathian foreland. Sedimentary Geology 343, 165–189.
Matoshko, A., Matoshko, A., de Leeuw, A., 2019. The Plio-Pleistocene demise of the East Carpathian foreland fluvial system and arrival of the paleo-Danube to the Black Sea. Geologica Carpathica 70, 91–112.
Meisch, C., 2000. Freshwater Ostracoda of Western and Central Europe. Spectrum Academicher Verlag, Heidelberg-Berlin.
MolluscaBase (Ed.), 2023. MolluscaBase, https://www.molluscabase.org (accessed on 2023-01-03).
Mullender, T.A., Frederichs, T., Hilgenfeldt, C., de Groot, L.V., Fabian, K., Dekkers, M.J., 2016. Automated paleomagnetic and rock magnetic data acquisition with an in-line horizontal “2 G” system. Geochemistry, Geophysics, Geosystems 17, 3546–3559.
Munteanu, I., Matenco, L., Dinu, C., Cloetingh, S., 2012. Effects of large sea-level variations in connected basins: the Dacian-Black Sea system of the eastern Paratethys. Basin Research 24, 583–597.
Nevesskaja, L.A., Popov, S.V., Goncharova, I.A., Guzhov, A.V., Yanin, B.T., Polubotko, I. V., Biakov, A.S., Gavrilova, V.A., 2013. Phanerozoic Bivalvia of Russia and adjacent countries. Transactions of the Paleontological Institute 294. Scientific World, Moscow.
Nevesskaja, L.A., Goncharova, I.A., Ilyina, L.B., Paramonova, N.P., Popov, S.V., Babak, E.V., Bagdasarjan, K.G., Voronina, A.A., 1986. Istorija neogenovych mollyuskov Paratetisa [History of the Neogene mollusks of Paratethys]. Nauka, Moskva (in Russian).
Nevesskaja, L.A., Paramonova, N.P., Babak, E.V., 1997. Opredelitel pliotsenovykh dvustvorchatykh mollyuskov yugo-zapadnoy Evrazii [Identification guide of bivalve mollusks of the Pliocene of south-western Eurasia]. Nauka, Moskva (in Russian).
Nevesskaja, L.A., Paramonova, N.P., Popov, S.V., 2001. History of Lymnocardiinae (Bivalvia, Cardiidae). Paleontological Journal 35, S146–S217.
Olteanu, R., 1979. Signification biostratigraphique des ostracodes méotiens et pontiens du Bassin Dacique. Revue roumain de géologie, géophysique et géographie, Série de géologie 23, 77–88.
Olteanu, R., 1989. The “Cîmpia Moment” (Late Miocene, Romania) and the Pannonian-Pontian boundary, defined by ostracods. Journal of Micropaleontology 8, 239–247.
Olteanu, R., 1989b. La faune d’ostracodes pontiens du Bassin Dacique. In: Stevanovič, P. Nevesskaja, L.A., Marinescu, Fl, Sokač, A., Jámbor, Á. (Eds.), Chronostratigraphie und Neostratotypen: Neogen der Westlichen (“Zentrale”) Paratethys 8. Pontien. Jazu and Sanu, Zagreb–Beograd, pp. 722–752.
Olteanu, R., 1995. Dacian ostracods. In: Marinescu, F., Papaianopol, I. (Eds.), Pliozän Pl1 Dazien. Chronostratigraphie und Neostratotypen. Neogen der Zentrale Paratethys. Editura Academiei Române, Bucharest, 530 p.
Olteanu R., 2006. Paleoecologia ecosistemelor salmastre din Bazinul Dacic. Evoluția paleogeografică și paleoecologică a arealului carpato-ponto-caspic în intervalul Miocen-Recent. Ecosisteme fosile. GeoEcoMar, Bucharest, 90 p.
Palcu, D.V., Krijgsman, W., 2022. The dire straits of Paratethys: Gateways to the anoxic giant of Eurasia. Geological Society London, Special Publications, p. 523.
Palcu, D.V., Patina, I.S., Șandric, I., Lazarev, S., Vasiliev, I., Stoica, M., Krijgsman, W., 2021. Late Miocene megalake regressions in Eurasia. Science Reports 11, 1–12.
Pană, I., Enache, C., Andreescu, I., 1981. Fauna de moluste a depozitelor cu ligniti din Oltenia. Institutul de cercetări, inginerie tehnologică și proiectări miniere pentru lignit Craiova, Craiova.
Papaianopol, I., 1975. Studiul unor taxoni ai genului *Chartoconcha* Andrussow din Pliocenul bazinului Dacic si importanta lor biostratigraphica. Dari de seama ale sedintelor, Institutul de geologie si Geofizica. Paleontologie 61 (3), 125–148.
Papaianopol, I., 1981. L’étude des Pontalmyres du bassin Dacique 30, 5–69.
Papaianopol, I., 1983. L’étude des espèces d’Euxinicardium du Pontien et Dacien du Bassin Dacique 31, 177–236.
Papaianopol, I., 1984. Nouveaux taxons de *Prosodacna* et *Psilodon (Prosodacn*a, Limnocardiidae, Bivalvia) du Pontien et du Dacien du bassin Dacique. Dari de seama ale sedintelor 68, 97–111.
Papaianopol, I., 1989. Considération sur les mollusques pontiens de Roumanie. In: Stevanovic, P., Nevesskaja, L.A., Marinescu, F., Sokac, A., Jambor, Á. (Eds.), Chronostratigraphie und Neostratotypen: Neogen der Westlichen (“Zentrale”) Paratethys 8. Pontien. Jazu-Sanu, Zagreb-Beograd, pp. 582–617.
Papaianopol, I., 1995. Faune de mollusques daciens du Bassin Dacique. In: Marinescu, F., Papaianopol, I. (Eds.), Chronostratigraphie und Neostratotypen, Bd. IX, Pl1. Dacien. Editura Academiei Române, Bucuresti, pp. 130–267.
Piller, W.E., Harzhauser, M., Mandic, O., 2007. Miocene Central Paratethys stratigraphy–current status and future directions. Stratigraphy 4, 151–168.
Popov, S.V., Rögl, F., Rozanov, A.Y., Steininger, F.F., Shcherba, I.G., Kovac, M. (Eds.), 2004. Lithological-Paleogeographic maps of Paratethys. Late Eocene to Pliocene. Courier Forschungsinstitut Senckenberg, Band 250, Frankfurt am Main.
Popov, S.V., Shcherba, I.G., Ilyina, L.B., Nevesskaya, L.A., Paramonova, N.P., Khondkarian, S.O., Magyar, I., 2006. Late Miocene to Pliocene palaeogeography of the Paratethys and its relation to the Mediterranean. Palaeogeography Palaeoclimatology Palaeoecology 238, 91–106.
Popov, S.V., Antipov, M.P., Zastrozhnov, A.S., Kurina, E.E., Pinchuk, T.N., 2010. Sea-level fluctuations on the northern shelf of the Eastern Paratethys in the Oligocene-Neogene. Stratigraphy and Geological Correlation 18, 200–224.
Popov, S.V., Rostovtseva, Y.V., Fillippova, N.Y., Golovina, L.A., Radionova, E.P., Goncharova, I.A., Vernyhorova, Y.V., Dykan, N.I., Pinchuk, T.N., Iljina, L.B., Koromyslova, A.V., Kozyrenko, T.M., Nikolaeva, I.A., Viskova, L.A., 2016. Paleontology and Stratigraphy of the Middle-Upper Miocene of the Taman Peninsula: Part 1. Description of Key Sections and Benthic Fossil Groups. Paleontological Journal 50, 1039–1206.
Popov, S.V., Rostovtseva, Y.V., Pinchuk, T.N., Patina, I.S., Goncharova, I.A., 2019. Oligocene to Neogene paleogeography and depositional environments of the Euxinian part of Paratethys in Crimean – Caucasian junction. Marine and Petroleum Geology 103, 163–175.
Radionova, E.P., Golovina, L.A., 2011. Upper Maeotian-lower Pontian “transitional strata” in the Taman peninsula: stratigraphic position and paleogeographic interpretation. Geologica Carpathica 62, 77–90.
Raffi, I., Wade, B.S., Pälike, H., Beu, A.G., Cooper, R., Crundwell, M.P., Krijgsman, W., Moore, T., Raine, I., Sardella, R., Vernyhorova, Y.V., 2020. The Neogene period. In: Gradstein, F.M., Ogg, J.G., Schmitz, M.D., Ogg, G.M. (Eds.), Geologic time scale 2020. Elsevier, pp. 1141–1215.
Rausch, L., Stoica, M., Lazarev, S., 2020. A late Miocene – early Pliocene paratethyan type ostracod fauna from the Denizli Basin (SW Anatolia) and its palaeogeographic implications. Acta Palaeontologica Romaniae 16, 3–56.
Reading, H.G. (Ed.), 1996. Sedimentary environments: processes, facies and stratigraphy. Blackwell Science.
Richards, K., van Christiaan, G.C., Baak, C.G.C., Athersuch, J., Hoyle, T.M., Stoica, M., Austin, W.E.N., Cage, A.G., Wonders, A.A.H., Marret, F., Pinnington, C.A., 2018. Palynology and micropalaeontology of the Pliocene - Pleistocene transition in outcrop from the western Caspian Sea, Azerbaijan: Potential links with the Mediterranean, Black Sea and the Arctic Ocean? Palaeogeography Palaeoclimatology Palaeoecology 511, 119–143.
Rögl, F., 1998. Palaeogeographic considerations for Mediterranean and Paratethys seaways. Annalen des Naturhistorischen Museums Wien 99A, 279–310.
Rostovtseva, Y.V., Rybkina, A.I., 2017. The Messinian event in the Paratethys: astronomical tuning of the Black Sea Pontian. Marine and Petroleum Geology 80, 321–332.
Rostovtseva, Y.V., Tesakova, E.M., 2009. Late Miocene Ostracodes (Ostracoda, Crustacea) from the Enikal Strait (Eastern Paratethys) as Indicators of Salinity Changes. Paleontological Journal 43, 170–177.
Roveri, M., Flecker, R., Krijgsman, W., Lofi, J., Lugli, S., Manzi, V., Sierro, F.J., Bertini, A., Camerlenghi, A., De Lange, G., Govers, R., Hilgen, F.J., Hübscher, C., Meijer, P. T., Stoica, M., 2014. The Messinian salinity crisis: past and future of a great challenge for marine sciences. Marine Geology 352, 25–58.
Schneider, G.F., 1949. Miotsenovaia fauna ostracod Kavkaza i Kryma [Miocene ostracod fauna of Caucasus and Crimea] 34, 89–179 (in Russian).
Schweyer, A.V., 1949. Ob Ostracoda pliotsena Severnogo Kavkaz ai Nizhnego Povolzhia s nekotorymi novymi dannymi k sistematike iskopaemykh ostracod [On the Pliocene ostracoda of the northern Caucasus and lower Volga region with some new data on the systematics of fossil ostracods]. Trudy V.N.I.G.R.I. 30, 7–68 (in Russian).
Snel, E., Marunteanu, M., Macalet, M., Meulenkamp, J.E., van Vugt, N., 2006. Late Miocene to Early Pliocene chronostratigraphic framework for the Dacic Basin, Romania. Palaeogeography Palaeoclimatology Palaeoecology 238, 107–124.
Sokač, A., 1972. Pannonian and Pontian ostracode fauna of Mt. Medvednica. Palaeontology Jugoslavija 2, 1–140.
Sokač, A., 1989. Pontian ostracod fauna in the Pannonian Basin. In: Stevanovič, P. Nevesskaja, L.A., Marinescu, Fl, Sokač, A., Jámbor, Á. (Eds.), Chronostratigraphie und Neostratotypen: Neogen der Westlichen (“Zentrale”) Paratethys 8. Pontien, Jazu and Sanu, Zagreb–Beograd, pp. 672–721.
Spadi, M., Gliozzi, E., Boomer, I., Stoica, M., Athersuch, J., 2019. Taxonomic harmonization of Neogene and Quaternary candonid genera (Crustacea, Ostracoda) of the Paratethys. Journal of Systematic Palaeontology 17, 1665–1698.
Stancheva, M., 1968. New data on the subfamily Leptocytherinae Hanai, 1957. Bulgarian Academy of Sciences, Bulletin of the Geological Institute 17, 37–48.
Stancheva, M., 1990. Upper Miocene ostracods from northern Bulgaria. Geologica Balcanica 5, 1–116.
Stefanescu S., 1896. Études sur les terrains tertiaires de Roumanie. Contributions à l’étude des faunes sarmatiques, pontiques et levantines. Mémoire de la Société Géologique de France, Paléontologie 15.
Stevanović, P., Nevesskaja, L.A., Marinescu, F., Sokač, A., Jambor, Á., 1989. Chronostratigraphie und Neostratotypen: Neogen der Westlichen (“Zentrale”) Paratethys 8. Pontien. Jazu-Sanu, Zagreb-Beograd.
Stoica, M., Lazar, I., Vasiliev, I., Krijgsman, W., 2007. Mollusc assemblages of the Pontian and Dacian deposits from the Topolog-Argeş area (southern Carpathian foredeep – Romania). Geobios 40, 391–405.

Stoica, M., Lazăr, I., Krijgsman, W., Vasiliev, I., Jipa, D., Floroiu, A., 2013. Paleoenvironmental evolution of the East Carpathian foredeep during the late Miocene–early Pliocene (Dacian Basin; Romania). Global and Planetary Change 103, 135–148.
Stoica, M., Krijgsman, W., Fortuin, A., Gliozzi, E., 2016. Paratethyan ostracods in the Spanish Lago-Mare: more evidence for interbasinal exchange at high Mediterranean Sea level. Palaeogeography Palaeoclimatology Palaeoecology 441, 854–870.
Suzin, A.V., 1956. Ostrakody tretichnykh otlozhenii Severnogo Predkavkazia [Ostracodes in the Tertiary Deposits of Northern Ciscaucasia]. Gostoptekhizdat, Moscow (in Russian).
Sztanó, O., Szafián, P., Magyar, I., Horányi, A., Bada, G., Hughes, D.W., Hoyer, D.L., Wallis, R.J., 2013. Aggradation and progradation controlled clinothems and deep-water sand delivery model in the Neogene Lake Pannon, Makó Trough, Pannonian Basin, SE Hungary. Global and Planetary Change 103, 149–167.
Tărăpoancă, M., Bertotti, G., Maţenco, L., Dinu, C., Cloetingh, S.A.P.L., 2003. Architecture of the Focşani depression: a 13 km deep basin in the Carpathians bend zone (Romania). Tectonics 22, 1074.
Tauxe, L., 2010. Essentials of Paleomagnetism. University of California Press, Berkely, Los Angeles, London.
ter Borgh, M., Stoica, M., Donselaar, M.E., Matenco, L., Krijgsman, W., 2014. Miocene connectivity between the Central and Eastern Paratethys: Constraints from the western Dacian Basin. Palaeogeography Palaeoclimatology Palaeoecology 412, 45–67.
ter Borgh, M., Radivojevic, D., Matenco, L., 2015. Constraining forcing factors and relative sea-level fluctuations in semi-enclosed basins: the late Neogene demise of Lake Pannon. Basin Research 27, 681–695.
Trubikhin, V.M., 1989. Paleomagnetic data for the Pontian. In: Stevanovic, P. M., Nevesskaja, L. A., Marinescu, Fl., Sokac, A., Jámbor, Á. (Eds.), Chronostratigraphie und Neostratotypen. Neogen der Westlichen (“Zentrale”) Paratethys VIII, Pl1, Pontien. Jazu-Sanu, Zagreb-Beograd, pp. 76–79.
Van Baak, C.G.C., Mandic, O., Lazar, I., Stoica, M., Krijgsman, W., 2015. The Slanicul de Buzau section, a unit stratotype for the Romanian stage of the Dacian Basin (Plio-Pleistocene, eastern Paratethys). Palaeogeography Palaeoclimatology Palaeoecology 440, 594–613.
Van Baak, C.G.C., Stoica, M., Grothe, A., Aliyeva, E., Krijgsman, W., 2016a. Mediterranean-Paratethys connectivity during the Messinian salinity crisis: the Pontian of Azerbaijan. Global and Planetary Change 141, 63–81.
Van Baak, C.G., Vasiliev, I., Palcu, D.V., Dekkers, M.J., Krijgsman, W., 2016b. A greigite-based magnetostratigraphic time frame for the Late Miocene to Recent DSDP Leg 42B cores from the Black Sea. Frontiers in Earth Science 4, 60.
Van Baak, C.G., Krijgsman, W., Magyar, I., Sztanó, O., Golovina, L.A., Grothe, A., Hoyle, T.M., Mandic, O., Patina, I.S., Popov, S.V., Radionova, E.P., Stoica, M., Vasiliev, I., 2017. Paratethys response to the Messinian salinity crisis. Earth-Science Reviews 172, 193–223.
Vasiliev, I., Krijgsman, W., Langereis, C.G., Panaiotu, C.E., Maţenco, L., Bertotti, G., 2004. Towards an astrochronological framework for the eastern ParatethysMio–Pliocene sedimentary sequences of the Focşani basin (Romania). Earth and Planetary Science Letters 227, 231–247.
Vasiliev, I., Krijgsman, W., Stoica, M., Langereis, C.G., 2005. Mio-Pliocene magnetostratigraphy in the southern Carpathian foredeep and Mediterranean-Paratethys correlations. Terra Nova 17 (4), 376–384.
Vasiliev, I., Iosifidi, A.G., Khramov, A.N., Krijgsman, W., Kuiper, K., Langereis, C.G., Popov, V.V., Stoica, M., Tomsha, V.A., Yudin, S.V., 2011. Magnetostratigraphy and radio-isotope dating of upper Miocene–lower Pliocene sedimentary successions of the Black Sea Basin (Taman Peninsula, Russia). Palaeogeography Palaeoclimatology Palaeoecology 310, 163–175.
Vasiliev, I., Reichart, G.J., Krijgsman, W., 2013. Impact of the Messinian Salinity Crisis on Black Sea hydrology – insights from hydrogen isotopes analysis on biomarkers. Earth and Planetary Science Letters 362, 272–282.
Vasiliev, I., Reichart, G.J., Grothe, A., Damsté, J.S.S., Krijgsman, W., Sangiorgi, F., Weijersa, J.W.H., van Roij, L., 2015. Recurrent phases of drought in the upper Miocene of the Black Sea region. Palaeogeography Palaeoclimatology Palaeoecology 423, 18–31.
Vasiliev, I., Stoica, M., Grothe, A., Lazarev, S., Palcu, D.V., van Baak, C., De Leeuw, A., Sangiorgi, F., Reichart, G.J., Davies, G.R., Krijgsman, W., 2021. Hydrological Changes in Restricted Basins: Insights From Strontium Isotopes on Late Miocene-Pliocene Connectivity of the Eastern Paratethys (Dacian Basin, Romania). Geochemistry, Geophysics, Geosystems 22, 1–18.
Vekua, M.L., 1975. Ostrakody kimeriiskikh i kuyalnitskikh otlozhenii Abkhazii i ikh stratigraficheskoe znachenie [The ostracods of the Kimmerian and Kujalinikian deposits of Abkhazia and their stratigraphic significance]. Academia Nauc Gruzinskoi SSR Ed, Metzniereba, Tibilisi (in Russian).
Wenz, W., 1942. Die Mollusken des Pliozäns der rumänischen Erdöl-Gebiete als Leitversteinerungen für die Aufschluss-Abeiten. Senckenbergiana 24, 1–293.
Wilke, T., Rolán, E., Davis, G.M., 2000. The mudsnail genus Hydrobia s.s. in the northern Atlantic and western Mediterranean: a Phylogenetic hypothesis. Marina Biology 137, 827–833.
Williams, L.R., Hiscott, R.N., Aksu, A.E., Bradley, L.R., Horne, D.J., Stoica, M., 2018. Holocene paleoecology and paleoceanography of the southwestern Black Sea shelf revealed by ostracod assemblages. Marine Micropaleontology 142, 48–66.
Yassini, I., 1986. Ecology, paleoecology and stratigraphy of ostracodes from Upper Pliocene and Quaternary deposits of the South Caspian Sea, North Irna. Lake Illawarra Management Committee, p. 78.